

OPTIMISTIC LIMITS OF THE COLORED JONES POLYNOMIALS AND THE COMPLEX VOLUMES OF HYPERBOLIC LINKS

JINSEOK CHO

(Received 2 September 2014; accepted 10 October 2015; first published online 14 March 2016)

Communicated by B. Martin

Abstract

The optimistic limit is a mathematical formulation of the classical limit, which is a physical method to estimate the actual limit by using the saddle-point method of a certain potential function. The original optimistic limit of the Kashaev invariant was formulated by Yokota, and a modified formulation was suggested by the author and others. This modified version is easier to handle and more combinatorial than the original one. On the other hand, it is known that the Kashaev invariant coincides with the evaluation of the colored Jones polynomial at a certain root of unity. This optimistic limit of the colored Jones polynomial was also formulated by the author and others, but it is very complicated and needs many unnatural assumptions. In this article, we suggest a modified optimistic limit of the colored Jones polynomial, following the idea of the modified optimistic limit of the Kashaev invariant, and show that it determines the complex volume of a hyperbolic link. Furthermore, we show that this optimistic limit coincides with the optimistic limit of the Kashaev invariant modulo $4\pi^2$. This new version is easier to handle and more combinatorial than the old version, and has many advantages over the modified optimistic limit of the Kashaev invariant. Because of these advantages, several applications have already appeared and more are in preparation.

2010 *Mathematics subject classification*: primary 57M27; secondary 51M25, 58J28.

Keywords and phrases: volume conjecture, optimistic limit, colored Jones polynomial, complex volume.

1. Introduction

For a hyperbolic link L , the volume conjecture, proposed by Kashaev in [11], claims the following nontrivial relation:

$$2\pi \lim_{N \rightarrow \infty} \frac{\log |\langle L \rangle_N|}{N} = \text{vol}(L),$$

The author is supported by the Basic Science Research Program through the National Research Foundation of Korea (NRF) funded by the Ministry of Education (2014047764 and NRF-2015R1C1A1A02037540).

© 2016 Australian Mathematical Publishing Association Inc. 1446-7887/2016 \$16.00

where $\text{vol}(L)$ is the hyperbolic volume of the link complement $\mathbb{S}^3 \setminus L$ and $\langle L \rangle_N$ is the N th Kashaev invariant. This conjecture is interesting because it relates geometric aspects of L with the quantum invariants. Some believe that it is a hint to a deeper connection between geometric and quantum topologies. (See [13], for example.) After that, the generalized conjecture was proposed in [16] that

$$2\pi i \lim_{N \rightarrow \infty} \frac{\log \langle L \rangle_N}{N} \equiv i(\text{vol}(L) + i \text{cs}(L)) \pmod{\pi^2},$$

where $\text{cs}(L)$ is the Chern–Simons invariant of $\mathbb{S}^3 \setminus L$ defined modulo π^2 in [21]. This conjecture is now called *the (generalized) volume conjecture* and $\text{vol}(L) + i \text{cs}(L)$ is called *the complex volume* of L .

When the volume conjecture was firstly proposed in [11], Kashaev considered *the classical limit* of the Kashaev invariant and verified his conjecture for three examples. The classical limit is a method of mathematical physics to estimate the actual limit by using the saddle-point method of a certain potential function. Although the behavior of the classical limit looks amazing, it cannot be well defined due to the ambiguity of the choice of the potential function. Therefore, Yokota suggested a combinatorial method to define the potential function in [20] and showed that some saddle point of his potential function determines the hyperbolic volume. This method was named *the optimistic limit* in [14] and developed by several authors in [8, 19].

Recently, the author together with H. Kim and S. Kim suggested a modified optimistic limit of any link diagram in [4] by using a slightly different potential function. Compared with the previous definition in [19], this new definition is easy to handle and has a natural geometric meaning. (We will summarize the results of [4] in Section 5.) Furthermore, the new definition has several applications to the quantum dilogarithm function in [9], the quandle theory in [2] and the cluster algebra in [10]. (The application to the cluster algebra of [10] will be discussed in the author's later article.)

On the other hand, the Kashaev invariant was proved to be the special value of the colored Jones polynomial in [15] as follows:

$$J_L\left(N; \exp \frac{2\pi i}{N}\right) = \langle L \rangle_N,$$

where $\langle L \rangle_N$ is the N th Kashaev invariant of a link L and $J_L(N; x)$ is the N th colored Jones polynomial of L with the complex variable x . The optimistic limit of the colored Jones polynomial, which uses a different potential function from the Kashaev invariant version, was firstly proposed in [17] and developed in [5, 6]. However, the general method developed in [6] is very complicated and needs several unnatural assumptions. In this article, we will suggest a modified optimistic limit of the colored Jones polynomial using the idea of [4]. This modified definition, which uses a slightly different potential function from [6], shares the same advantages of the definition in [4], namely it is easy to handle and has a natural geometric meaning.

The two optimistic limits of the Kashaev invariant and the colored Jones polynomial are almost the same in many ways. Although they use different potential functions,

which are denoted by $V(z_1, \dots, z_g)$ and $W(w_1, \dots, w_n)$, respectively, and slightly different subdivisions of the same octahedral decomposition, the resulting values are the same complex volume. (The potential function $W(w_1, \dots, w_n)$ will be defined in Section 2.) However, due to the difference of the subdivision, the colored Jones polynomial version has a wonderful advantage that the set of equations

$$\mathcal{I} := \left\{ \exp\left(w_k \frac{\partial W}{\partial w_k}\right) = 1 \mid k = 1, \dots, n \right\} \quad (1.1)$$

always has solutions for any diagram of the hyperbolic link L . As a matter of fact, for any given boundary-parabolic representation $\rho : \pi_1(L) \rightarrow \mathrm{PSL}(2, \mathbb{C})$ of the link group $\pi_1(L) := \pi_1(\mathbb{S}^3 \setminus L)$ and for any link diagram D , we can construct a solution of \mathcal{I} that induces the representation ρ . (This is proved in one of the author's later articles [1].) The optimistic limit of the Kashaev invariant has a similar property, which is proved in [2], but some diagrams cannot have any solution. See Figure 13 in Section 5, for an example.

The existence of solutions for any link diagram is a very useful property because, by using it, we can study the hyperbolic structure of the link combinatorially. This approach already has several interesting applications, for example [1, 3, 7], and more applications are in preparation.

The set of hyperbolicity equations consists of the gluing equations and the completeness condition of a certain triangulation. In the case of \mathcal{I} , it is related to an ideal triangulation of $\mathbb{S}^3 \setminus (L \cup \{\text{two points}\})$, which will be defined in Section 3. We name it *the five-term triangulation* and the two removed points in \mathbb{S}^3 are denoted by $\pm\infty$. The exact relationship between the five-term triangulation and the set \mathcal{I} is the following proposition.

PROPOSITION 1.1. *For a hyperbolic link L with a fixed diagram, consider the potential function $W(w_1, \dots, w_n)$ of the diagram. Then the set \mathcal{I} defined in (1.1) becomes the set of the hyperbolicity equations associated with the five-term triangulation of $\mathbb{S}^3 \setminus (L \cup \{\pm\infty\})$.*

We remark that Proposition 1.1 was essentially proved in [6, Section 4]. However, the proof in [6] is very long and complicated, and what we need is only part of it, so we will sketch the proof of Proposition 1.1 in Section 3 for the reader's convenience.

Note that many parts of this article overlap with the author's previous article [6]. However, the major difference is that we are using triangulation of $\mathbb{S}^3 \setminus (L \cup \{\pm\infty\})$, whereas the previous work used triangulation of $\mathbb{S}^3 \setminus L$. Therefore, when we proved some properties in [6], we first considered the general case and then proceeded to the special cases when certain edges or faces of the triangulation are collapsed to vertices. (There are many special cases and it requires many unnatural assumptions on link diagrams.) However, in this article, the proofs of the general case in [6] are good enough and these remove almost all technical difficulties of the previous work. This is the major reason to develop this new version.

Let $\mathcal{T} = \{(w_1, \dots, w_n)\}$ be the set of solutions¹ of \mathcal{I} in \mathbb{C}^n . Then, according to the results in [1], we know that $\mathcal{T} \neq \emptyset^2$. By [18, Theorem 1], all edges in the five-term triangulation are essential. (An essential edge roughly means that it is not null-homotopic. See [18] for the exact definition.) Therefore, for a solution $\mathbf{w} \in \mathcal{T}$, we can construct the boundary-parabolic representation

$$\rho_{\mathbf{w}} : \pi_1(\mathbb{S}^3 \setminus (L \cup \{\pm\infty\})) = \pi_1(\mathbb{S}^3 \setminus L) \longrightarrow \text{PSL}(2, \mathbb{C}), \tag{1.2}$$

using Yoshida’s construction in [12, Section 4.5]. (The solution $\mathbf{w} \in \mathcal{T}$ satisfies the completeness condition, so $\rho_{\mathbf{w}}$ is boundary-parabolic.) Note that the volume $\text{vol}(\rho_{\mathbf{w}})$ and the Chern–Simons invariant $\text{cs}(\rho_{\mathbf{w}})$ of $\rho_{\mathbf{w}}$ were defined in [21]. We call $\text{vol}(\rho_{\mathbf{w}}) + i \text{cs}(\rho_{\mathbf{w}})$ the complex volume of $\rho_{\mathbf{w}}$.

For the solution set $\mathcal{T} \subset \mathbb{C}^n$, let \mathcal{T}_j be a path component of \mathcal{T} satisfying $\mathcal{T} = \cup_{j \in J} \mathcal{T}_j$ for the index set J . We assume that $0 \in J$ for notational convenience. To obtain well-defined values from the potential function $W(w_1, \dots, w_n)$, we slightly modify it to

$$W_0(w_1, \dots, w_n) := W(w_1, \dots, w_n) - \sum_{k=1}^n \left(w_k \frac{\partial W}{\partial w_k} \right) \log w_k. \tag{1.3}$$

Then the main result of this article follows.

THEOREM 1.2. *Let L be a hyperbolic link with a fixed diagram, $W(w_1, \dots, w_n)$ be the potential function of the diagram and $\mathcal{T} = \cup_{j \in J} \mathcal{T}_j$ be the solution set of \mathcal{I} . Then, for any $\mathbf{w} \in \mathcal{T}_j$, $W_0(\mathbf{w})$ is constant (it depends only on j) and*

$$W_0(\mathbf{w}) \equiv i(\text{vol}(\rho_{\mathbf{w}}) + i \text{cs}(\rho_{\mathbf{w}})) \pmod{\pi^2}, \tag{1.4}$$

where $\rho_{\mathbf{w}}$ is the boundary-parabolic representation obtained in (1.2). Furthermore, there exists a path component \mathcal{T}_0 of \mathcal{T} satisfying

$$W_0(\mathbf{w}_{\infty}) \equiv i(\text{vol}(L) + i \text{cs}(L)) \pmod{\pi^2}$$

for any $\mathbf{w}_{\infty} \in \mathcal{T}_0$.

The proof will be given in Section 4. The main idea is to use Zickert’s formula of the extended Bloch group in [21]. Although this idea was already used in [4] and several other places, this proof has not appeared anywhere before.

We call the value $W_0(\mathbf{w})$ the optimistic limit of the colored Jones polynomial. Note that it depends on the choice of the diagram and the path component \mathcal{T}_j .

¹We only consider solutions satisfying the condition that, when the potential function is expressed by $W(w_1, \dots, w_n) = \sum \pm \text{Li}_2(w) + (\text{extra terms})$, the variables inside the dilogarithms satisfy $w \notin \{0, 1, \infty\}$. Previously, in [6, 19], these solutions were called essential solutions.

²The article [1] depends on this article, so using $\mathcal{T} \neq \emptyset$ may look illogical. However, the proof of it in [1] relies only on Proposition 1.1 of this article and it does not require the fact that $\mathcal{T} \neq \emptyset$. Furthermore, all results in this article still work well if we just assume $\mathcal{T} \neq \emptyset$.

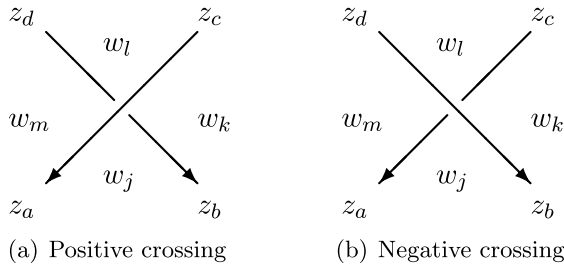


FIGURE 1. Assignment of variables.

The optimistic limit of the Kashaev invariant, defined in [4], will be surveyed in Section 5. The potential function $V(z_1, \dots, z_g)$ is defined from the diagram D of the hyperbolic link L , and the set of equations

$$\mathcal{H} := \left\{ \exp\left(z_k \frac{\partial V}{\partial z_k}\right) = 1 \mid k = 1, \dots, g \right\}$$

becomes the set of the hyperbolicity equations associated with the four-term triangulation. Four-term triangulation is obtained from the same octahedron of the five-term triangulation by subdividing it into four tetrahedra. Therefore, four-term triangulation is also a triangulation of $\mathbb{S}^3 \setminus (L \cup \{\pm\infty\})$.

Although both sets of the hyperbolicity equations \mathcal{I} and \mathcal{H} are based on the same octahedron decomposition of $\mathbb{S}^3 \setminus (L \cup \{\pm\infty\})$, these two sets look quite different. The variables w_1, \dots, w_n of \mathcal{I} are assigned to regions of the link diagram D , but z_1, \dots, z_g of \mathcal{H} are assigned to sides of D . (See Figure 1.) Furthermore, the equations in \mathcal{I} are all gluing equations and they induce the completeness condition, whereas the equations in \mathcal{H} are all completeness conditions along the meridian and they induce the gluing equations. The author feels that these two definitions of the optimistic limits seem to be dual to each other.

Let $\mathcal{S} = \{(z_1, \dots, z_g)\}$ be the set of solutions of \mathcal{H} in \mathbb{C}^g . Then, for a solution $\mathbf{z} \in \mathcal{S}$, we can obtain the boundary-parabolic representation

$$\rho_{\mathbf{z}} : \pi_1(\mathbb{S}^3 \setminus (L \cup \{\pm\infty\})) = \pi_1(\mathbb{S}^3 \setminus L) \longrightarrow \text{PSL}(2, \mathbb{C}).$$

Now we modify the potential function V to

$$V_0(z_1, \dots, z_g) := V(z_1, \dots, z_g) - \sum_{k=1}^g \left(z_k \frac{\partial V}{\partial z_k} \right) \log z_k.$$

Then the main result of [4] can be summarized to the following identity:

$$V_0(\mathbf{z}) \equiv i(\text{vol}(\rho_{\mathbf{z}}) + i \text{cs}(\rho_{\mathbf{z}})) \pmod{\pi^2}. \tag{1.5}$$

From (1.4) and (1.5), we can easily see that, if $\rho_{\mathbf{w}} = \rho_{\mathbf{z}}$, then

$$W_0(\mathbf{w}) \equiv V_0(\mathbf{z}) \pmod{\pi^2}.$$

This result is formulated in a stronger form as follows.

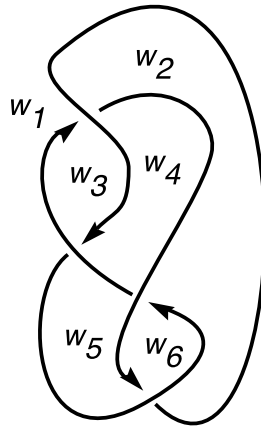


FIGURE 2. The figure-eight knot 4_1 .

THEOREM 1.3. Assume that the diagram D of the hyperbolic link L does not have a kink. For a solution $\mathbf{w} \in \mathcal{T}$, if the variables w_j, \dots, w_m in Figure 1 satisfy

$$w_j + w_l \neq w_k + w_m$$

at all crossings, then there exists a solution $\mathbf{z} \in \mathcal{S}$ satisfying

$$\rho_{\mathbf{w}} = \rho_{\mathbf{z}} \quad \text{and} \quad W_0(\mathbf{w}) \equiv V_0(\mathbf{z}) \pmod{4\pi^2}. \quad (1.6)$$

Inversely, for a solution $\mathbf{z} \in \mathcal{S}$, there always exists a solution $\mathbf{w} \in \mathcal{T}$ satisfying (1.6).

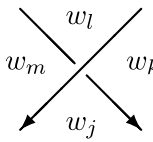
The proof of Theorem 1.3 essentially appeared in [6]. However, it is based on very long and complicated calculations, and what we need here is only some parts of them. So, we will sketch the proof of Theorem 1.3 in Section 6 for the reader's convenience.

In Section 7, we will apply Theorem 1.3 to the example of twist knots and show several numerical calculations. Finally, in Appendix A, we will discuss the invariance of the optimistic limit under the change of signs of the variables of the potential function. This property will be used in the author's later article.

2. Potential function $W(w_1, \dots, w_n)$

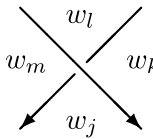
Consider a hyperbolic link L and its oriented diagram D . We define *sides* of D by the arcs connecting two adjacent crossing points¹. For example, the diagram of the figure-eight knot 4_1 in Figure 2 has eight sides. Also, we define *regions* of D by the regions surrounded by sides. For example, the diagram in Figure 2 has six regions.

¹Most people use the word *edge* instead of *side* here. However, in this paper, we want to keep the word *edge* for the edge of a tetrahedron.



$$\begin{aligned} W_P := & -\text{Li}_2\left(\frac{w_l}{w_m}\right) - \text{Li}_2\left(\frac{w_l}{w_k}\right) + \text{Li}_2\left(\frac{w_j w_l}{w_k w_m}\right) \\ & + \text{Li}_2\left(\frac{w_m}{w_j}\right) + \text{Li}_2\left(\frac{w_k}{w_j}\right) - \frac{\pi^2}{6} + \log \frac{w_m}{w_j} \log \frac{w_k}{w_j} \end{aligned}$$

(a) Positive crossing



$$\begin{aligned} W_N := & \text{Li}_2\left(\frac{w_l}{w_m}\right) + \text{Li}_2\left(\frac{w_l}{w_k}\right) - \text{Li}_2\left(\frac{w_j w_l}{w_k w_m}\right) \\ & - \text{Li}_2\left(\frac{w_m}{w_j}\right) - \text{Li}_2\left(\frac{w_k}{w_j}\right) + \frac{\pi^2}{6} - \log \frac{w_m}{w_j} \log \frac{w_k}{w_j} \end{aligned}$$

(b) Negative crossing

FIGURE 3. Potential functions of the crossings.

We assign complex variables w_1, \dots, w_n to each region of the diagram D . Using the dilogarithm function $\text{Li}_2(w) = -\int_0^w (\log(1-t)/t) dt$, we define the potential function¹ of a crossing as in Figure 3.

Note that this potential function comes from the formal substitution of the R-matrix of the colored Jones polynomial. Refer to [6] for details.

The potential function $W(w_1, \dots, w_n)$ of the diagram D is defined by the summation of all potential functions of the crossings. For example, the potential function of the figure-eight knot 4_1 in Figure 2 is

$$\begin{aligned} W(w_1, \dots, w_6) &= \left\{ -\text{Li}_2\left(\frac{w_1}{w_3}\right) - \text{Li}_2\left(\frac{w_1}{w_2}\right) + \text{Li}_2\left(\frac{w_1 w_4}{w_2 w_3}\right) + \text{Li}_2\left(\frac{w_3}{w_4}\right) \right. \\ &\quad \left. + \text{Li}_2\left(\frac{w_2}{w_4}\right) - \frac{\pi^2}{6} + \log \frac{w_3}{w_4} \log \frac{w_2}{w_4} \right\} \\ &\quad + \left\{ -\text{Li}_2\left(\frac{w_4}{w_3}\right) - \text{Li}_2\left(\frac{w_4}{w_5}\right) + \text{Li}_2\left(\frac{w_1 w_4}{w_3 w_5}\right) + \text{Li}_2\left(\frac{w_3}{w_1}\right) \right. \\ &\quad \left. + \text{Li}_2\left(\frac{w_5}{w_1}\right) - \frac{\pi^2}{6} + \log \frac{w_3}{w_1} \log \frac{w_5}{w_1} \right\} \\ &\quad + \left\{ \text{Li}_2\left(\frac{w_2}{w_4}\right) + \text{Li}_2\left(\frac{w_2}{w_6}\right) - \text{Li}_2\left(\frac{w_2 w_5}{w_4 w_6}\right) - \text{Li}_2\left(\frac{w_4}{w_5}\right) \right\} \end{aligned}$$

¹Note that, by using \approx to denote the equivalence relation in [6, Lemma 3.1], we know that

$$\log \frac{w_j}{w_m} \log \frac{w_j}{w_k} \approx (\log w_j - \log w_m)(\log w_j - \log w_k) \approx \log \frac{w_m}{w_j} \log \frac{w_k}{w_j}.$$

Therefore, changing $\log(w_j/w_m) \log(w_j/w_k)$ of W_N to $\log(w_m/w_j) \log(w_k/w_j)$ does not have any effect on \mathcal{I} and the optimistic limit. To avoid redundant calculation, we will use $\log(w_j/w_m) \log(w_j/w_k)$ up to Section 4 and change it to $\log(w_m/w_j) \log(w_k/w_j)$ in Section 6.

$$\begin{aligned}
 & - \operatorname{Li}_2\left(\frac{w_6}{w_5}\right) + \frac{\pi^2}{6} - \log \frac{w_4}{w_5} \log \frac{w_6}{w_5} \Big\} \\
 & + \left\{ \operatorname{Li}_2\left(\frac{w_5}{w_1}\right) + \operatorname{Li}_2\left(\frac{w_5}{w_6}\right) - \operatorname{Li}_2\left(\frac{w_2 w_5}{w_1 w_6}\right) - \operatorname{Li}_2\left(\frac{w_1}{w_2}\right) \right. \\
 & \left. - \operatorname{Li}_2\left(\frac{w_6}{w_2}\right) + \frac{\pi^2}{6} - \log \frac{w_1}{w_2} \log \frac{w_6}{w_2} \right\}.
 \end{aligned}$$

We define a modified potential function $W_0(w_1, \dots, w_n)$ as in (1.3). Recall that \mathcal{I} was defined in (1.1) and \mathcal{T} is the set of solutions of \mathcal{I} in \mathbb{C}^n . Also, recall that we are considering the solutions $\mathbf{w} = (w_1, \dots, w_n) \in \mathbb{C}^n$ of \mathcal{I} with the property that if the potential function is expressed by $W(w_1, \dots, w_n) = \sum \pm \operatorname{Li}_2(w) + (\text{extra terms})$, then variables inside the dilogarithms satisfy $w \notin \{0, 1, \infty\}$.

Note that the functions $\operatorname{Li}_2(w)$ and $\log w$ are multi-valued functions. Therefore, to obtain well-defined values, we have to select the proper branch of the logarithm by choosing $\arg w$ and $\arg(1 - w)$. The following lemma, which corresponds to [4, Lemma 2.1], shows why we consider the potential function W_0 instead of W .

LEMMA 2.1. *Let $\mathbf{w} = (w_1, \dots, w_n) \in \mathcal{T}$. For the potential function $W(w_1, \dots, w_n)$, the value of $W_0(\mathbf{w})$ is invariant under any choice of branch of the logarithm modulo $4\pi^2$.*

PROOF. Note that it was almost proved in [4, Lemma 2.1]. Using the idea in [4], we can write down

$$W_0^*(\mathbf{w}) - W_0(\mathbf{w}) \equiv \sum_{k=1}^n \left\{ -\left(w_k \frac{\partial W}{\partial w_k}\right) \log^* w_k + \left(w_k \frac{\partial W}{\partial w_k}\right) \log w_k \right\} \pmod{4\pi^2}, \tag{2.1}$$

where $W^*(\mathbf{w})$ and $\log^* w$ are the functions with different log-branches corresponding to an analytic continuation of $W(\mathbf{w})$ and $\log w$, respectively. We already assumed that that $\mathbf{w} = (w_1, \dots, w_n) \in \mathcal{T}$, so

$$\left(w_k \frac{\partial W}{\partial w_k}\right) \log^* w_k \equiv \left(w_k \frac{\partial W}{\partial w_k}\right) \log w_k \pmod{4\pi^2},$$

and (2.1) is zero modulo $4\pi^2$. □

The following lemma and corollary already appeared in [4] and were proved as Lemma 2.2 and Corollary 2.3, respectively. (Substituting $V, V_0, \mathcal{H}, \mathcal{S}_j$ and z_k in the proof of [4] by $W, W_0, \mathcal{I}, \mathcal{T}_j$ and w_k , respectively, gives the proof.)

LEMMA 2.2. *Let $\mathcal{T} = \cup_{j \in J} \mathcal{T}_j \subset \mathbb{C}^n$ be the solution set of \mathcal{I} with \mathcal{T}_j being a path component. Assume that $\mathcal{T} \neq \emptyset$. Then, for any $\mathbf{w} = (w_1, \dots, w_n) \in \mathcal{T}_j$,*

$$W_0(\mathbf{w}) \equiv C_j \pmod{4\pi^2},$$

where C_j is a complex constant depending only on $j \in J$.

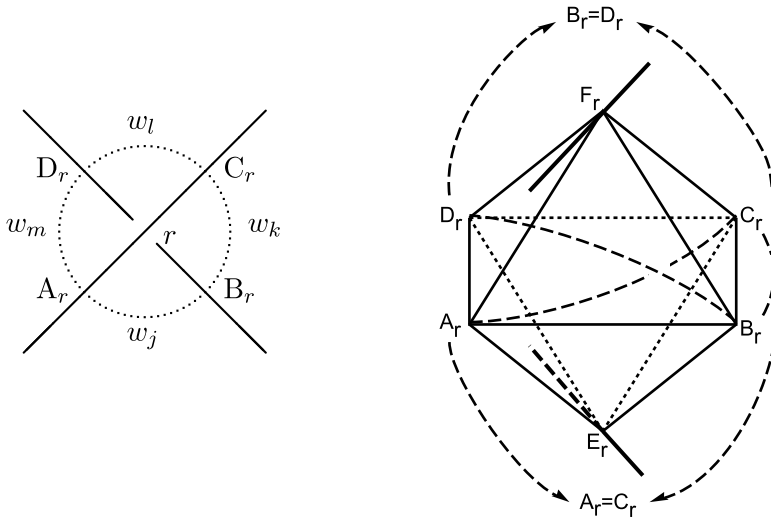


FIGURE 4. Octahedron on the crossing r .

COROLLARY 2.3. *If $\mathbf{w} = (w_1, \dots, w_n) \in \mathcal{T}_j$, then*

$$\lambda \mathbf{w} := (\lambda w_1, \dots, \lambda w_n) \in \mathcal{T}_j$$

for any nonzero complex number λ . Furthermore,

$$W_0(\mathbf{w}) \equiv W_0(\lambda \mathbf{w}) \pmod{4\pi^2}.$$

Due to Corollary 2.3, we can consider the solution set \mathcal{T} as a subset of $\mathbb{C}P^{n-1}$ instead of \mathbb{C}^n .

3. Five-term triangulation of $\mathbb{S}^3 \setminus (L \cup \{\pm\infty\})$

In this section, we describe the five-term triangulation of $\mathbb{S}^3 \setminus (L \cup \{\text{two points}\})$. We remark that this triangulation was previously named Thurston triangulation in [6].

We place an octahedron $A_r B_r C_r D_r E_r F_r$ on each crossing r of the link diagram as in Figure 4 so that the vertices A_r and C_r lie on the over-bridge and the vertices B_r and D_r on the under-bridge of the diagram, respectively. Then we twist the octahedron by gluing edges $B_r F_r$ to $D_r F_r$ and $A_r E_r$ to $C_r E_r$, respectively. The edges $A_r B_r$, $B_r C_r$, $C_r D_r$ and $D_r A_r$ are called *horizontal edges* and we sometimes express these edges in the diagram as arcs around the crossing on the left-hand side of Figure 4.

Then we glue faces of the octahedra following the sides of the diagram. Specifically, there are three gluing patterns as in Figure 5. In each case (a), (b) and (c), we identify the faces $\triangle A_r B_r E_r \cup \triangle C_r B_r E_r$ to $\triangle C_{r+1} D_{r+1} F_{r+1} \cup \triangle C_{r+1} B_{r+1} F_{r+1}$, $\triangle B_r C_r F_r \cup \triangle D_r C_r F_r$ to $\triangle D_{r+1} C_{r+1} F_{r+1} \cup \triangle B_{r+1} C_{r+1} F_{r+1}$ and $\triangle A_r B_r E_r \cup \triangle C_r B_r E_r$ to $\triangle C_{r+1} B_{r+1} E_{r+1} \cup \triangle A_{r+1} B_{r+1} E_{r+1}$, respectively. We call (a) *alternating gluings* and (b) and (c) *nonalternating gluings*.

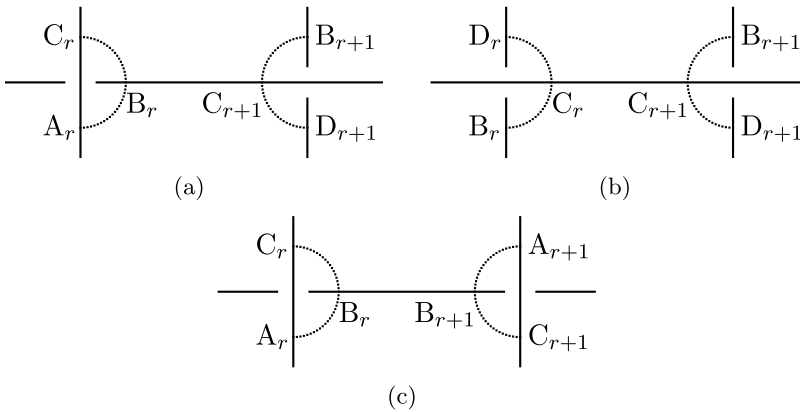


FIGURE 5. Three gluing patterns.

Note that this gluing process identifies vertices $\{A_r, C_r\}$ to one point, denoted by $-\infty$, and $\{B_r, D_r\}$ to another point, denoted by ∞ , and finally $\{E_r, F_r\}$ to the other points, denoted by P_j , where $j = 1, \dots, s$ and s is the number of the components of the link L . The regular neighborhoods of $-\infty$ and ∞ are 3-balls and that of $\cup_{j=1}^s P_j$ is a tubular neighborhood of the link L . Therefore, if we remove the vertices P_1, \dots, P_s from the octahedra, then we obtain a decomposition of $\mathbb{S}^3 \setminus L$, denoted by T . On the other hand, if we remove all the vertices of the octahedra, the result becomes an ideal decomposition of $\mathbb{S}^3 \setminus (L \cup \{\pm\infty\})$. We call the latter *the octahedral decomposition* and denote it by T' .

To obtain an ideal triangulation from T' , we divide each octahedron $A_r B_r C_r D_r E_r F_r$ in Figure 4 into five ideal tetrahedra $A_r B_r D_r F_r$, $B_r C_r D_r F_r$, $A_r B_r C_r D_r$, $A_r B_r C_r E_r$ and $A_r C_r D_r E_r$. We call the result *the five-term triangulation* of $\mathbb{S}^3 \setminus (L \cup \{\pm\infty\})$. On the other hand, if we divide the same octahedron into four ideal tetrahedra $A_r B_r E_r F_r$, $B_r C_r E_r F_r$, $C_r D_r E_r F_r$ and $D_r A_r E_r F_r$, then the result is called *the four-term triangulation*. The four-term triangulation was used in [4] and will appear again in Sections 5 and 6 of this article.

Note that if we assign the shape parameter $u \in \mathbb{C} \setminus \{0, 1\}$ to an edge of an ideal hyperbolic tetrahedron, then the other edges are also parameterized by $u, u' := 1/(1-u)$ and $u'' := 1 - (1/u)$ as in Figure 6.

To determine the shape of the octahedron in Figure 4, we assign shape parameters to edges of tetrahedra as in Figure 7. Note that both of $(w_j w_l)/(w_k w_m)$ in Figure 7(a) and $(w_k w_m)/(w_j w_l)$ in Figure 7(b) are the shape parameters of the tetrahedron $A_r B_r C_r D_r$ assigned to the edges $B_r D_r$ and $A_r C_r$. Also, note that the assignment of shape parameters here does not depend on the orientations of the link diagram.

To obtain the boundary parabolic representation $\pi_1(\mathbb{S}^3 \setminus (L \cup \{\pm\infty\})) \rightarrow \text{PSL}(2, \mathbb{C})$, we require two conditions on the ideal triangulation of $\mathbb{S}^3 \setminus (L \cup \{\pm\infty\})$; the product of shape parameters on any edge in the triangulation becomes one, and the holonomies induced by meridian and longitude of the torus cusps act as translations on the torus

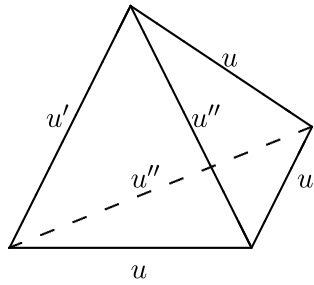


FIGURE 6. Parameterization of an ideal tetrahedron with a shape parameter u .

cusped. Note that these conditions are expressed as equations of shape parameters. The former equations are called *(Thurston's) gluing equations*, the latter is called the *completeness condition* and the whole set of these equations are called *the hyperbolicity equations*. As already discussed in [4] and Section 1, a solution \mathbf{w} of the hyperbolicity equation determines a boundary-parabolic representation

$$\rho_{\mathbf{w}} : \pi_1(\mathbb{S}^3 \setminus (L \cup \{\pm\infty\})) = \pi_1(\mathbb{S}^3 \setminus L) \longrightarrow \mathrm{PSL}(2, \mathbb{C}).$$

The rest of this section is devoted to the proof of Proposition 1.1. It was already proved¹ in [6], so we sketch the proof here.

PROOF (SKETCH OF THE PROOF OF PROPOSITION 1.1). For all the crossings of the link diagram and the corresponding octahedra in Figure 4, let \mathcal{A} be the set of horizontal edges $A_r B_r, B_r C_r, C_r D_r$ and $D_r A_r$. Let \mathcal{B} be the set of edges $B_r F_r, D_r F_r, A_r E_r, C_r E_r$ of all crossings and other edges glued to them. Let \mathcal{C} be the set of edges $A_r C_r$ and $B_r D_r$ of all crossings. Finally, let \mathcal{D} be the set of all the other edges in the triangulation. Note that if the link diagram is alternating, then $\mathcal{D} = \emptyset$.

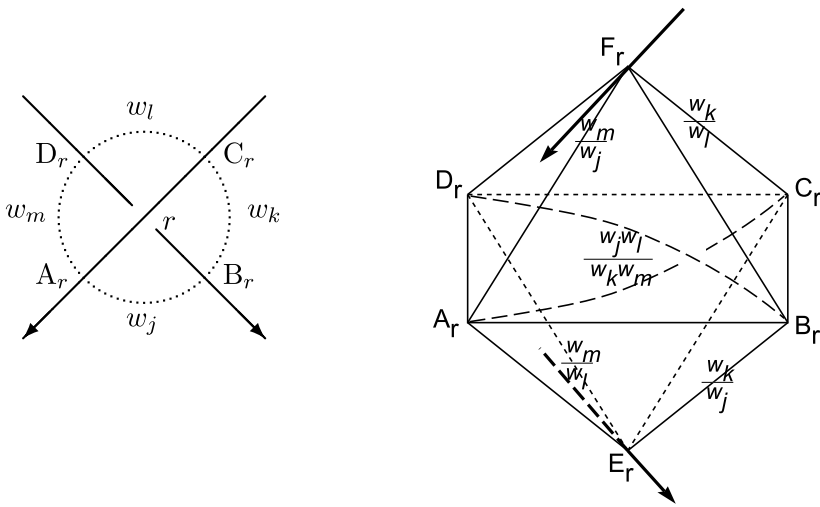
Recall that W_P and W_N are the potential functions defined in Figure 3. Direct calculation shows that $\exp(w_a(\partial W_P / \partial w_a))$ for $a = j, k, l, m$ is the product of the shape parameters assigned to the horizontal edge corresponding to the region w_a in Figure 7(a). For example,

$$\exp\left(w_j \frac{\partial W_P}{\partial w_j}\right) = \left(\frac{w_j w_l}{w_k w_m}\right)' \left(\frac{w_m}{w_j}\right)'' \left(\frac{w_k}{w_j}\right)'',$$

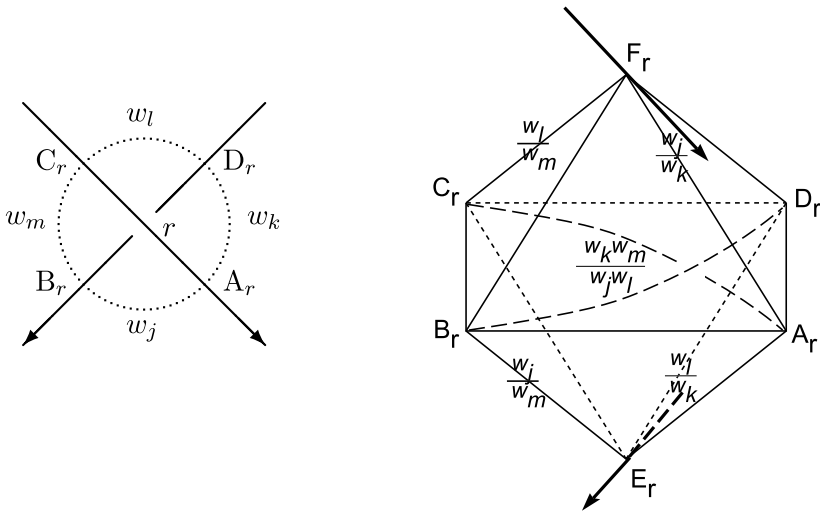
which is the product of the shape parameters assigned to the edge $A_r B_r$. (See [6, (8)–(10)] for the other equations. In [6], our W_P and W_N were denoted by P_1 and N_1 , respectively.) Furthermore, the same holds for $\exp(w_a(\partial W_N / \partial w_a))$, too. Therefore, \mathcal{I} becomes the gluing equations of the edges in \mathcal{A} .

The gluing equations of the edges in \mathcal{C} and \mathcal{D} hold trivially because of the assigning rule of the shape parameters to the tetrahedra. We will show that the gluing equations

¹The proof is in [6, Lemma 4.1 and Proposition 1.1], which started from the general case and then proceeded to the collapsed cases. In this article, the collapsed cases do not happen, so the general case is enough.



(a) Positive crossing



(b) Negative crossing

FIGURE 7. Assignment of shape parameters.

of the edges in \mathcal{B} hold trivially, too. Consider the alternating gluing in Figure 8(a). This induces a part of the cusp diagram as in Figure 8(b), which comes from the gluing of two tetrahedra in Figure 8(c). On the other hand, the nonalternating gluings in Figure 5(b) and (c) do not have any effect on the cusp diagram of the torus cusp.

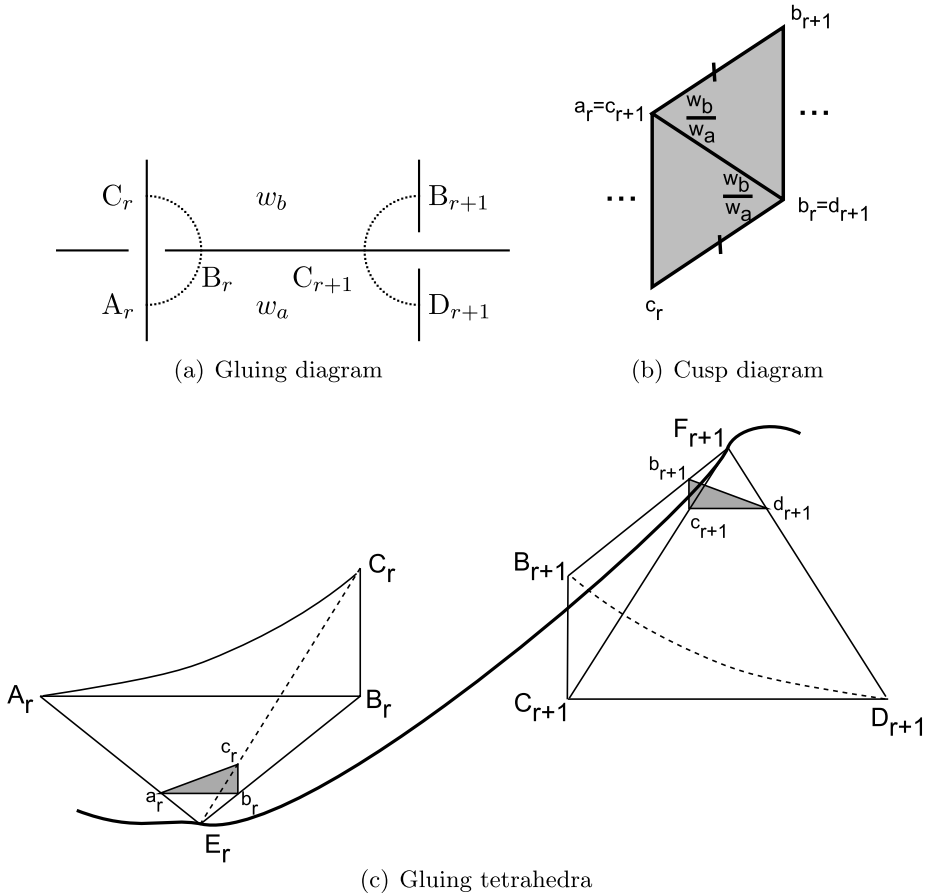


FIGURE 8. Cusp diagram induced from Figure 5(a).

Note that the cusp diagram in Figure 8(b) is an annulus because the edge $c_{r+1}b_{r+1}$ is identified with $c_r b_r$. The shape parameter w_b/w_a is assigned to the edges $B_r E_r$ and $C_{r+1} F_{r+1}$ in Figure 8(c), and the product of shape parameters on the edge $B_r E_r = B_{r+1} F_{r+1} = D_{r+1} F_{r+1} \in \mathcal{B}$ (around the vertex $b_r = b_{r+1} = d_{r+1}$ in Figure 8(b)) is

$$\frac{w_b}{w_a} \left(\frac{w_b}{w_a} \right)'' \left(\frac{w_b}{w_a} \right)' = -1.$$

Therefore, if we consider another annulus on the right-hand side of the edge $b_{r+1} d_{r+1}$ in Figure 8(b), the gluing equation of the edge $B_r E_r = B_{r+1} F_{r+1} = D_{r+1} F_{r+1} \in \mathcal{B}$ is satisfied trivially.

The other gluing equations of the edges in \mathcal{B} can be obtained in the same way. Hence, we conclude that \mathcal{I} induces the gluing equations of all the edges in $\mathcal{A} \cup \mathcal{B} \cup \mathcal{C} \cup \mathcal{D}$. Furthermore, the cusp diagram in Figure 8(b) already satisfies one

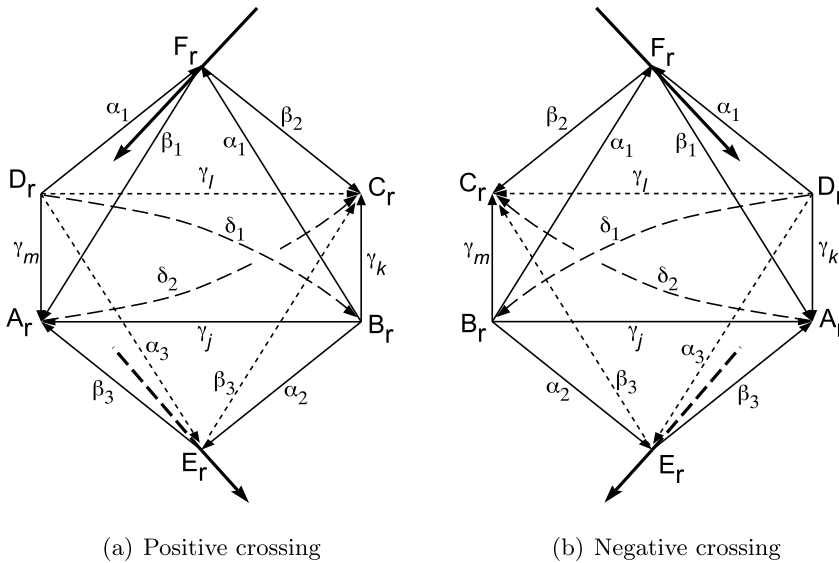


FIGURE 9. Vertex orderings and labelings of edges.

completeness condition of the meridian that sends the edge $c_r b_r$ to $c_{r+1} b_{r+1}$. Therefore, \mathcal{I} induces all the hyperbolicity equations. \square

4. Proof of Theorem 1.2

In this section, we always assume that $\mathbf{w} = (w_1, \dots, w_n)$ is a solution in \mathcal{T} . The main technique of the proof of Theorem 1.2 is the extended Bloch group theory in [21]. To apply it, we first define the vertex ordering of the five-term triangulation in Figure 9 so that the order 0, 1, 2 and 3 is assigned to the vertices of each tetrahedra in the order of $D_r B_r F_r A_r$, $B_r E_r A_r C_r$, $D_r B_r F_r C_r$, $D_r E_r A_r C_r$ and $D_r B_r A_r C_r$.

Note that the vertex ordering of each tetrahedron induces the orientations of the edges and the tetrahedron. The induced orientation of the tetrahedron can be different from the original orientation induced by the triangulation. For example, this is the case for the tetrahedra $D_r B_r F_r C_r$ and $D_r E_r A_r C_r$ in Figure 9(a) and $D_r B_r F_r A_r$, $B_r E_r A_r C_r$ and $D_r B_r A_r C_r$ in Figure 9(b). If the two orientations are the same, we define the sign of the tetrahedron $\sigma = 1$ and, if they are different, then $\sigma = -1$.

One important property of our vertex orientation is that when two edges are glued together in the triangulation, the orientations of the two edges induced by each vertex ordering coincide. (We call this condition *edge-orientation consistency*.) Because of this property, we can apply the formula in [21].

The five-term triangulation we are using is an ideal triangulation, so we parameterized all ideal tetrahedra of the triangulation by assigning shape parameters as in Figure 7. For each tetrahedron with the vertex orientation, we define an element

of the extended pre-Bloch group $\sigma[u^\sigma; p, q] \in \widehat{\mathcal{P}}(\mathbb{C})$, where σ is the sign of the tetrahedron, u is the shape parameter assigned to the edge connecting the zeroth and first vertices and p, q are certain integers.

Zickert suggested a way to determine p and q from the developing map of the representation $\rho : \pi_1(M) \rightarrow \text{PSL}(2, \mathbb{C})$ of a hyperbolic manifold M in [21], and showed that

$$\sum \sigma \widehat{L}([u^\sigma; p, q]) \equiv i(\text{vol}(\rho) + i \text{cs}(\rho)) \pmod{\pi^2}, \tag{4.1}$$

where the summation is over all tetrahedra and

$$\widehat{L}([u; p, q]) = \text{Li}_2(u) - \frac{\pi^2}{6} + \frac{1}{2}q\pi i \log u + \frac{1}{2}(p\pi i + \log u) \log(1 - u)$$

is a complex-valued function defined on $\widehat{\mathcal{P}}(\mathbb{C})$.

Although our five-term triangulation is for $\mathbb{S}^3 \setminus (L \cup \{\pm\infty\})$, the formula of [21] is still valid because we can consider the two points $\pm\infty$ as interior points of the manifold $\mathbb{S}^3 \setminus L$. To apply the formula, we have to remove the interior vertices, which results in our five-term triangulation of $\mathbb{S}^3 \setminus (L \cup \{\pm\infty\})$. (See [21, Theorem 4.11] for details.)

Here, we remark that the author made a mistake in his previous article [4] when justifying the usage of the triangulation of $\mathbb{S}^3 \setminus (L \cup \{\pm\infty\})$. He mentioned Thurston’s spinning construction of [12], but it can be applied when a boundary-parabolic representation is already given, and the construction shows that the parameter space determines the volume of the representation, not the complex volume. (Note that [12, Lemma 2.3 and Proposition 3.1] are still valid for *any* boundary-parabolic representation and its volume. However, we cannot directly guarantee the invariance of the Chern–Simons invariant from [12].)

To determine p, q of $\sigma[u^\sigma; p, q]$ corresponding to each tetrahedron with vertex orientation, we assign certain complex numbers g_{jk} to the edge connecting the j th and k th vertices, where $j, k \in \{0, 1, 2, 3\}$ and $j < k$. We assume that g_{jk} satisfies the property that if two edges are glued together in the triangulation, then the assigned numbers g_{jk} of the glued edges coincide. We do not use the exact values of g_{jk} in this article, but remark that there is an explicit method in [21] for calculating these numbers using the developing map. With the given numbers g_{jk} , we can calculate p, q using the following equation, which appeared as [21, Equation (3.5)]:

$$\begin{cases} p\pi i = -\log u^\sigma + \log g_{03} + \log g_{12} - \log g_{02} - \log g_{13}, \\ q\pi i = \log(1 - u^\sigma) + \log g_{02} + \log g_{13} - \log g_{01} - \log g_{23}. \end{cases} \tag{4.2}$$

To avoid confusion, we use variables $\alpha_1, \alpha_2, \alpha_3, \beta_1, \beta_2, \beta_3, \gamma_j, \gamma_k, \gamma_l, \gamma_m, \delta_1$ and δ_2 instead of g_{jk} as in Figure 9. Note that γ_a ($a = j, k, l, m$) is assigned to the horizontal edge that lies in the region with w_a . The orientation we defined in Figure 9 satisfies the edge-orientation consistency, so we will apply the formula of [21] to our five-term triangulation.

For the positive crossing r in Figure 9(a), let $\sigma_1^{(r)}[u_1^{\sigma_1^{(r)}}; p_1^{(r)}, q_1^{(r)}], \dots, \sigma_5^{(r)}[u_5^{\sigma_5^{(r)}}; p_5^{(r)}, q_5^{(r)}]$ be the elements in $\widehat{\mathcal{P}}(\mathbb{C})$ corresponding to $D_r B_r F_r A_r, B_r E_r A_r C_r, D_r B_r F_r C_r, D_r E_r A_r C_r$ and $D_r B_r A_r C_r$, respectively. Then

$$\sigma_1^{(r)} = \sigma_2^{(r)} = \sigma_5^{(r)} = 1, \quad \sigma_3^{(r)} = \sigma_4^{(r)} = -1,$$

$$u_1^{\sigma_1^{(r)}} = \frac{w_m}{w_j}, \quad u_2^{\sigma_2^{(r)}} = \frac{w_k}{w_j}, \quad u_3^{\sigma_3^{(r)}} = \frac{w_l}{w_k}, \quad u_4^{\sigma_4^{(r)}} = \frac{w_l}{w_m}, \quad u_5^{\sigma_5^{(r)}} = \frac{w_j w_l}{w_k w_m},$$

and direct calculation from (4.2) shows that

$$\begin{cases} p_1^{(r)} \pi i + \log \frac{w_m}{w_j} = \log \gamma_m - \log \gamma_j, \\ p_2^{(r)} \pi i + \log \frac{w_k}{w_j} = \log \gamma_k - \log \gamma_j, \\ p_3^{(r)} \pi i + \log \frac{w_l}{w_k} = \log \gamma_l - \log \gamma_k, \\ p_4^{(r)} \pi i + \log \frac{w_l}{w_m} = \log \gamma_l - \log \gamma_m, \\ p_5^{(r)} \pi i + \log \frac{w_j w_l}{w_k w_m} = \log \gamma_j + \log \gamma_l - \log \gamma_k - \log \gamma_m \end{cases} \quad (4.3)$$

and

$$\begin{cases} q_1^{(r)} \pi i - \log \left(1 - \frac{w_m}{w_j}\right) = \log \alpha_1 + \log \gamma_j - \log \delta_1 - \log \beta_1, \\ q_2^{(r)} \pi i - \log \left(1 - \frac{w_k}{w_j}\right) = \log \gamma_j + \log \beta_3 - \log \alpha_2 - \log \delta_2, \\ q_3^{(r)} \pi i - \log \left(1 - \frac{w_l}{w_k}\right) = \log \alpha_1 + \log \gamma_k - \log \delta_1 - \log \beta_2, \\ q_4^{(r)} \pi i - \log \left(1 - \frac{w_l}{w_m}\right) = \log \gamma_m + \log \beta_3 - \log \alpha_3 - \log \delta_2, \\ q_5^{(r)} \pi i - \log \left(1 - \frac{w_j w_l}{w_k w_m}\right) = \log \gamma_m + \log \gamma_k - \log \delta_1 - \log \delta_2. \end{cases} \quad (4.4)$$

For the negative crossing r in Figure 9(b), let $\sigma_1^{(r)}[u_1^{\sigma_1^{(r)}}; p_1^{(r)}, q_1^{(r)}], \dots, \sigma_5^{(r)}[u_5^{\sigma_5^{(r)}}; p_5^{(r)}, q_5^{(r)}]$ be the elements in $\widehat{\mathcal{P}}(\mathbb{C})$ corresponding to $B_r E_r A_r C_r, D_r B_r F_r A_r, D_r E_r A_r C_r, D_r B_r F_r C_r$ and $D_r B_r A_r C_r$, respectively. Then

$$\sigma_1^{(r)} = \sigma_2^{(r)} = \sigma_5^{(r)} = -1, \quad \sigma_3^{(r)} = \sigma_4^{(r)} = 1,$$

$$u_1^{\sigma_1^{(r)}} = \frac{w_m}{w_j}, \quad u_2^{\sigma_2^{(r)}} = \frac{w_k}{w_j}, \quad u_3^{\sigma_3^{(r)}} = \frac{w_l}{w_k}, \quad u_4^{\sigma_4^{(r)}} = \frac{w_l}{w_m}, \quad u_5^{\sigma_5^{(r)}} = \frac{w_j w_l}{w_k w_m},$$

and direct calculation from (4.2) shows that

$$\begin{cases} p_1^{(r)} \pi i + \log \frac{w_m}{w_j} = \log \gamma_m - \log \gamma_j, \\ p_2^{(r)} \pi i + \log \frac{w_k}{w_j} = \log \gamma_k - \log \gamma_j, \\ p_3^{(r)} \pi i + \log \frac{w_l}{w_k} = \log \gamma_l - \log \gamma_k, \\ p_4^{(r)} \pi i + \log \frac{w_l}{w_m} = \log \gamma_l - \log \gamma_m, \\ p_5^{(r)} \pi i + \log \frac{w_j w_l}{w_k w_m} = \log \gamma_j + \log \gamma_l - \log \gamma_k - \log \gamma_m \end{cases} \tag{4.5}$$

and

$$\begin{cases} q_1^{(r)} \pi i - \log \left(1 - \frac{w_m}{w_j}\right) = \log \gamma_j + \log \beta_3 - \log \alpha_2 - \log \delta_2, \\ q_2^{(r)} \pi i - \log \left(1 - \frac{w_k}{w_j}\right) = \log \alpha_1 + \log \gamma_j - \log \delta_1 - \log \beta_1, \\ q_3^{(r)} \pi i - \log \left(1 - \frac{w_l}{w_k}\right) = \log \gamma_k + \log \beta_3 - \log \alpha_3 - \log \delta_2, \\ q_4^{(r)} \pi i - \log \left(1 - \frac{w_l}{w_m}\right) = \log \alpha_1 + \log \gamma_m - \log \delta_1 - \log \beta_2, \\ q_5^{(r)} \pi i - \log \left(1 - \frac{w_j w_l}{w_k w_m}\right) = \log \gamma_k + \log \gamma_m - \log \delta_1 - \log \delta_2. \end{cases} \tag{4.6}$$

From the above definitions, we can conclude that

$$\sum_{r: \text{crossings}} \sum_{c=1}^5 \sigma_c^{(r)} [u_c^{\sigma_c^{(r)}}; p_c^{(r)}, q_c^{(r)}] \in \widehat{\mathcal{P}}(\mathbb{C})$$

is the corresponding element of the five-term triangulation. The following observation can be easily obtained.

OBSERVATION 4.1. *There exists a constant C satisfying*

$$\log w_b \equiv \log \gamma_b + C \pmod{\pi i}$$

for all $b = 1, \dots, n$.

PROOF. The relation (4.3) or (4.5) holds for any crossing r of the link diagram. Therefore, by letting $C = \log w_1 - \log \gamma_1$, it follows trivially. \square

Now we define an integer $Q_a^{(r)}$ for the crossing r and $a = j, k, l, m$ in the following ways. For the positive crossing r in Figure 9(a), we define

$$\begin{cases} Q_j^{(r)} = q_1^{(r)} + q_2^{(r)} - q_5^{(r)} + p_1^{(r)} + p_2^{(r)}, \\ Q_k^{(r)} = -q_2^{(r)} - q_3^{(r)} + q_5^{(r)} - p_1^{(r)}, \\ Q_l^{(r)} = q_3^{(r)} + q_4^{(r)} - q_5^{(r)}, \\ Q_m^{(r)} = -q_4^{(r)} - q_1^{(r)} + q_5^{(r)} - p_2^{(r)} \end{cases} \tag{4.7}$$

and, for the negative crossing r in Figure 9(b), we define

$$\begin{cases} Q_j^{(r)} = -q_1^{(r)} - q_2^{(r)} + q_5^{(r)} - p_1^{(r)} - p_2^{(r)}, \\ Q_k^{(r)} = q_2^{(r)} + q_3^{(r)} - q_5^{(r)} + p_1^{(r)}, \\ Q_l^{(r)} = -q_3^{(r)} - q_4^{(r)} + q_5^{(r)}, \\ Q_m^{(r)} = q_4^{(r)} + q_1^{(r)} - q_5^{(r)} + p_2^{(r)}. \end{cases} \tag{4.8}$$

Note that, from the definitions (4.7) and (4.8), we can directly obtain

$$\sum_{a=j,k,l,m} Q_a^{(r)} = 0 \tag{4.9}$$

for any crossing r .

LEMMA 4.2. For the potential function $W(w_1, \dots, w_n)$ and the index $b = 1, \dots, n$,

$$w_b \frac{\partial W}{\partial w_b} = \sum_r Q_b^{(r)} \pi i,$$

where r is over the crossings that lie on the boundary of the region associated with w_b .

PROOF. Note that W_P and W_N were defined in Figure 3.

For the positive crossing r in Figure 9(a), direct calculation from (4.3) and (4.4) shows that

$$\begin{cases} w_j \frac{\partial W_P}{\partial w_j} = Q_j^{(r)} \pi i + (\log \beta_1 - \log \alpha_1) + (\log \alpha_2 - \log \beta_3), \\ w_k \frac{\partial W_P}{\partial w_k} = Q_k^{(r)} \pi i + (\log \alpha_1 - \log \beta_2) + (\log \beta_3 - \log \alpha_2), \\ w_l \frac{\partial W_P}{\partial w_l} = Q_l^{(r)} \pi i + (\log \beta_2 - \log \alpha_1) + (\log \alpha_3 - \log \beta_3), \\ w_m \frac{\partial W_P}{\partial w_m} = Q_m^{(r)} \pi i + (\log \alpha_1 - \log \beta_1) + (\log \beta_3 - \log \alpha_3). \end{cases}$$

For the negative crossing r in Figure 9(b), direct calculation from (4.5) and (4.6) shows that

$$\begin{cases} w_j \frac{\partial W_N}{\partial w_j} = Q_j^{(r)} \pi i + (\log \alpha_1 - \log \beta_1) + (\log \beta_3 - \log \alpha_2), \\ w_k \frac{\partial W_N}{\partial w_k} = Q_k^{(r)} \pi i + (\log \beta_1 - \log \alpha_1) + (\log \alpha_3 - \log \beta_3), \\ w_l \frac{\partial W_N}{\partial w_l} = Q_l^{(r)} \pi i + (\log \alpha_1 - \log \beta_2) + (\log \beta_3 - \log \alpha_3), \\ w_m \frac{\partial W_N}{\partial w_m} = Q_m^{(r)} \pi i + (\log \beta_2 - \log \alpha_1) + (\log \alpha_2 - \log \beta_3). \end{cases}$$

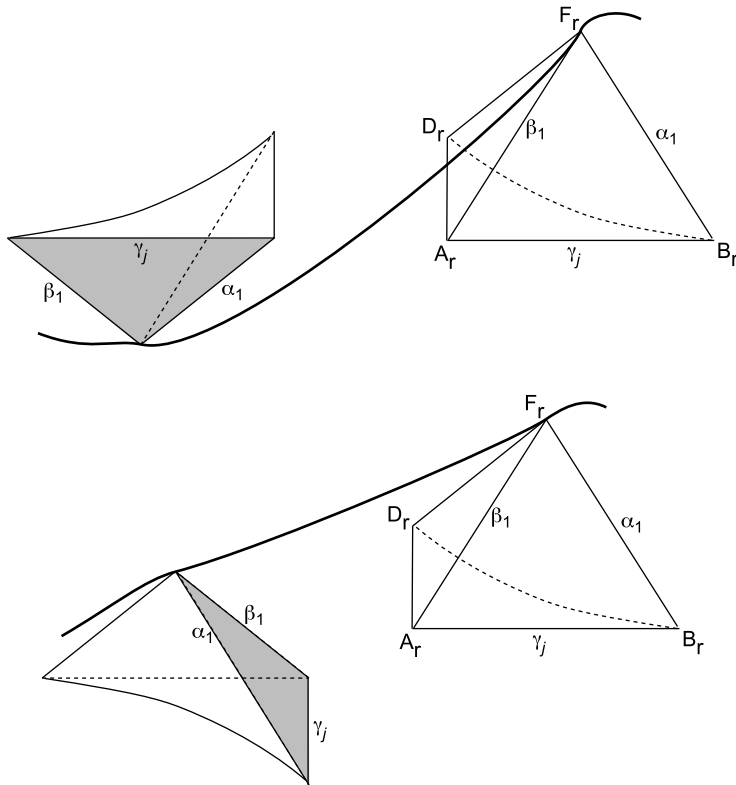


FIGURE 10. Two cases of the gluing of $A_r B_r F_r$.

From the above calculations, we can find a general rule. Elaborating on $w_j(\partial W_P / \partial w_j)$, consider the faces $A_r B_r F_r$ and $A_r B_r E_r$ in Figure 9(a). The term $(\log \beta_1 - \log \alpha_1)$ in $w_j(\partial W_P / \partial w_j)$ comes from the edges $A_r F_r$ and $B_r F_r$ of the face $A_r B_r F_r$, counterclockwise, and the term $(\log \alpha_2 - \log \beta_3)$ comes from the edges $B_r E_r$ and $A_r E_r$ of the face $A_r B_r E_r$ clockwise. These rules hold for all the cases.

Consider the face $A_r B_r F_r$ and its corresponding term $(\log \beta_1 - \log \alpha_1)$. As in Figure 10, the face glued to $A_r B_r F_r$ induces the term $(\log \alpha_1 - \log \beta_1)$, which cancels out the term corresponding to $A_r B_r F_r$. (The shaded faces in Figure 10 are glued to $A_r B_r F_r$.) In the same way, all the other terms corresponding to the other faces cancel each other and the proof follows. \square

By combining (4.9) and Lemma 4.2, or by direct calculation,

$$\sum_{b=1}^n w_b \frac{\partial W}{\partial w_b} = 0. \tag{4.10}$$

To obtain (1.4), we need to use (4.1) and prove that

$$W(w_1, \dots, w_n) - \sum_{b=1}^n \left(w_b \frac{\partial W}{\partial w_b} \right) \log w_b \equiv \sum_{r,c} \sigma_c^{(r)} \widehat{L}([u_c^{\sigma_c^{(r)}}; p_c^{(r)}, q_c^{(r)}]) \pmod{\pi^2}, \tag{4.11}$$

where $c = 1, \dots, 5$ and r is over all crossings. At first, from (4.7) and (4.8),

$$\begin{aligned} \sum_{a=j,k,l,m} Q_a^{(r)} \pi i \log w_a &\equiv -\sigma_1^{(r)} \left\{ q_1^{(r)} \pi i \log \frac{w_m}{w_j} + q_2^{(r)} \pi i \log \frac{w_k}{w_j} - q_3^{(r)} \pi i \log \frac{w_l}{w_k} \right. \\ &\quad \left. - q_4^{(r)} \pi i \log \frac{w_l}{w_m} + q_5^{(r)} \pi i \log \frac{w_j w_l}{w_k w_m} + p_1^{(r)} \pi i \log \frac{w_k}{w_j} + p_2^{(r)} \pi i \log \frac{w_m}{w_j} \right\} \\ &\equiv -\sum_{c=1}^5 \sigma_c^{(r)} q_c^{(r)} \pi i \log u_c^{\sigma_c^{(r)}} \\ &\quad - \sigma_1^{(r)} p_1^{(r)} \pi i \log u_2^{\sigma_2^{(r)}} - \sigma_1^{(r)} p_2^{(r)} \pi i \log u_1^{\sigma_1^{(r)}} \pmod{2\pi^2}. \end{aligned} \tag{4.12}$$

Combining (4.12) and Lemma 4.2,

$$\begin{aligned} \frac{1}{2} \sum_{r,c} \sigma_c^{(r)} q_c^{(r)} \pi i \log u_c^{\sigma_c^{(r)}} &\equiv -\frac{1}{2} \sum_{b=1}^n \left(w_b \frac{\partial W}{\partial w_b} \right) \log w_b \\ &\quad - \frac{1}{2} \sum_r \{ \sigma_1^{(r)} p_1^{(r)} \pi i \log u_2^{\sigma_2^{(r)}} + \sigma_1^{(r)} p_2^{(r)} \pi i \log u_1^{\sigma_1^{(r)}} \} \pmod{\pi^2}, \end{aligned} \tag{4.13}$$

where $c = 1, \dots, 5$ and r is over all crossings.

Let $W^{(r)}$ be the potential function of the crossing r , that is,

$$W^{(r)} := \begin{cases} W_P & \text{if } r \text{ is a positive crossing,} \\ W_N & \text{if } r \text{ is a negative crossing.} \end{cases}$$

From (4.3), (4.5) and direct calculation,

$$\begin{aligned} &\sum_{c=1}^5 \sigma_c^{(r)} (p_c^{(r)} \pi i + \log u_c^{\sigma_c^{(r)}}) \log(1 - u_c^{\sigma_c^{(r)}}) \\ &= \sigma_1^{(r)} \left\{ (\log \gamma_m - \log \gamma_j) \log \left(1 - \frac{w_m}{w_j} \right) + (\log \gamma_k - \log \gamma_j) \log \left(1 - \frac{w_k}{w_j} \right) \right. \\ &\quad \left. - (\log \gamma_l - \log \gamma_k) \log \left(1 - \frac{w_l}{w_k} \right) - (\log \gamma_l - \log \gamma_m) \log \left(1 - \frac{w_l}{w_m} \right) \right. \\ &\quad \left. + (\log \gamma_j + \log \gamma_l - \log \gamma_k - \log \gamma_m) \log \left(1 - \frac{w_j w_l}{w_k w_m} \right) \right\} \\ &= - \sum_{a=j,k,l,m} \log \gamma_a \left(w_a \frac{\partial W^{(r)}}{\partial w_a} \right) \\ &\quad + \sigma_1^{(r)} (\log \gamma_m - \log \gamma_j) \log \frac{w_k}{w_j} + \sigma_1^{(r)} (\log \gamma_k - \log \gamma_j) \log \frac{w_m}{w_j} \end{aligned}$$

$$\begin{aligned}
 &= - \sum_{a=j,k,l,m} \log \gamma_a \left(w_a \frac{\partial W^{(r)}}{\partial w_a} \right) \\
 &\quad + \sigma_1^{(r)} p_1^{(r)} \pi i \log u_2^{\sigma_2^{(r)}} + \sigma_1^{(r)} p_2^{(r)} \pi i \log u_1^{\sigma_1^{(r)}} + 2 \log \frac{w_k}{w_j} \log \frac{w_m}{w_j}. \tag{4.14}
 \end{aligned}$$

Using Observation 4.1, (4.10) and

$$w_b \frac{\partial W}{\partial w_b} \equiv 0 \pmod{2\pi i},$$

$$\begin{aligned}
 \sum_{r: \text{crossings}} \sum_{a=j,k,l,m} \log \gamma_a \left(w_a \frac{\partial W^{(r)}}{\partial w_a} \right) &= \sum_{b=1}^n \log \gamma_b \left(w_b \frac{\partial W}{\partial w_b} \right) \\
 &\equiv \sum_{b=1}^n \left(w_b \frac{\partial W}{\partial w_b} \right) \log w_b \pmod{2\pi^2}. \tag{4.15}
 \end{aligned}$$

From (4.13), (4.14) and (4.15),

$$\begin{aligned}
 &\frac{1}{2} \sum_{r,c} \sigma_c^{(r)} \{ q_c^{(r)} \pi i \log u_c^{\sigma_c^{(r)}} + (p_c^{(r)} \pi i + \log u_c^{\sigma_c^{(r)}}) \log(1 - u_c^{\sigma_c^{(r)}}) \} \\
 &\equiv - \sum_{b=1}^n \left(w_b \frac{\partial W}{\partial w_b} \right) \log w_b + \sum_r \log u_1^{\sigma_1^{(r)}} \log u_2^{\sigma_2^{(r)}} \pmod{\pi^2}, \tag{4.16}
 \end{aligned}$$

where $c = 1, \dots, 5$ and r is over all crossings.

By definition, the potential function $W(w_1, \dots, w_n)$ is expressed by

$$W(w_1, \dots, w_n) = \sum_{r,c} \sigma_c^{(r)} \left\{ \text{Li}_2(u_c^{\sigma_c^{(r)}}) - \frac{\pi^2}{6} \right\} + \sum_r \log u_1^{\sigma_1^{(r)}} \log u_2^{\sigma_2^{(r)}}. \tag{4.17}$$

From (4.16) and (4.17), we obtain (4.11) and complete the proof of the first part of Theorem 1.2.

On the other hand, the existence of \mathbf{w}_∞ is guaranteed by [12]. (See [4] for details. Or, if we allow the construction in [1], we can construct \mathbf{w}_∞ from the discrete faithful representation $\rho : \pi_1(L) \rightarrow \text{PSL}(2, \mathbb{C})$.) Then we can choose \mathcal{T}_0 , the path component containing \mathbf{w}_∞ . This completes the proof of Theorem 1.2.

5. The optimistic limit of the Kashaev invariant

To prove Theorem 1.3, we briefly review the results of [4].

Consider a hyperbolic link L and its nonoriented diagram D . (If D already has an orientation, then we ignore it.) Assume that D does not have any kinks¹ by removing them as in Figure 11.

¹This assumption is only for the optimistic limit of the Kashaev invariant. If the diagram has a kink, then the hyperbolicity equations in \mathcal{H} defined in (5.1) do not have any solution. On the other hand, the hyperbolicity equations in \mathcal{I} always have a solution whether it has a kink or not.

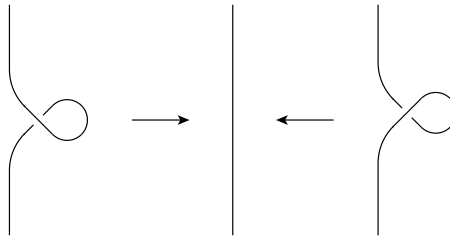


FIGURE 11. Removing kinks.

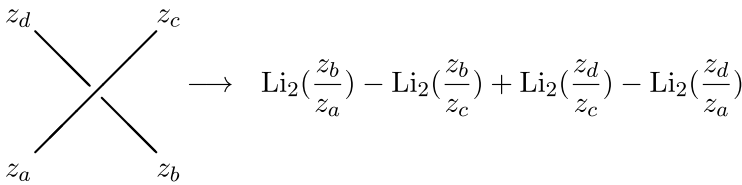


FIGURE 12. Potential function of a crossing.

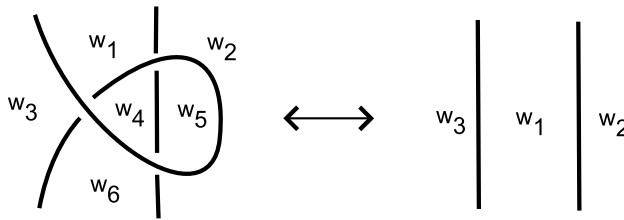


FIGURE 13. Diagram with $S = \emptyset$ and $\mathcal{T} \neq \emptyset$.

We assign complex variables z_1, \dots, z_g to sides of the diagram. Then we define the potential function of the crossing as in Figure 12.

The potential function $V(z_1, \dots, z_g)$ of the diagram D is defined by the summation of all potential functions of the crossings. Then we define the set \mathcal{H} by

$$\mathcal{H} := \left\{ \exp\left(z_k \frac{\partial V}{\partial z_k}\right) = 1 \mid k = 1, \dots, g \right\}. \tag{5.1}$$

Let $\mathcal{S} = \{(z_1, \dots, z_g)\}$ be the set of solutions¹ of \mathcal{H} in \mathbb{C}^g . We always assume that $\mathcal{S} \neq \emptyset$. Note that we cannot avoid this assumption because, if the diagram contains the left-hand side of Figure 13, then $\mathcal{S} = \emptyset$, but $\mathcal{T} \neq \emptyset$. (See [1, 4] for details.)

¹As already mentioned in Section 1, we only consider solutions satisfying the condition that, when the potential function V is expressed by $V(z_1, \dots, z_g) = \sum \pm \text{Li}_2(z_a/z_b)$, the variables inside the dilogarithms satisfy $z_a/z_b \notin \{0, 1, \infty\}$. Furthermore, for the crossing in Figure 14, the solution should satisfy $z_c/z_a \neq 1$ and $z_d/z_b \neq 1$. The latter condition, which the author missed in his previous paper [4], is needed to avoid the holonomies induced by the meridians becoming the trivial map.

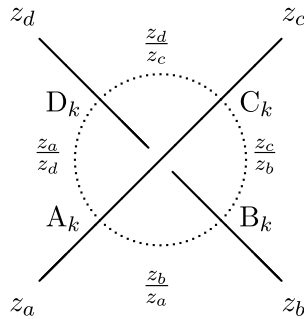


FIGURE 14. Parameterizing tetrahedra.

Recall that the four-term triangulation of $\mathbb{S}^3 \setminus (L \cup \{\pm\infty\})$ was defined in Section 2. To determine the shape of the tetrahedra, we assign shape parameters z_b/z_a , z_c/z_b , z_d/z_c and z_a/z_d to the horizontal edges A_kB_k , B_kC_k , C_kD_k and D_kA_k , respectively. (See Figure 14.) Then we obtain the following proposition, which was [4, Proposition 1.1].

PROPOSITION 5.1. *For a hyperbolic link L with a fixed diagram, consider the potential function $V(z_1, \dots, z_g)$ of the diagram. Then the set \mathcal{H} defined in (5.1) becomes the set of the hyperbolicity equations associated with the four-term triangulation of $\mathbb{S}^3 \setminus (L \cup \{\pm\infty\})$.*

By using Yoshida’s construction in [12, Section 4.5], for a solution $\mathbf{z} = (z_1, \dots, z_g) \in \mathcal{S}$, we can obtain a boundary-parabolic representation

$$\rho_{\mathbf{z}} : \pi_1(\mathbb{S}^3 \setminus (L \cup \{\pm\infty\})) = \pi_1(\mathbb{S}^3 \setminus L) \longrightarrow \text{PSL}(2, \mathbb{C}). \tag{5.2}$$

For the solution set \mathcal{S} , let \mathcal{S}_j be a path component of \mathcal{S} satisfying $\mathcal{S} = \cup_{j \in J'} \mathcal{S}_j$ for some index set J' . We assume that $0 \in J'$ for notational convenience. To obtain well-defined values from the potential function $V(z_1, \dots, z_g)$, we slightly modify it to

$$V_0(z_1, \dots, z_g) := V(z_1, \dots, z_g) - \sum_{k=1}^n \left(z_k \frac{\partial V}{\partial z_k} \right) \log z_k.$$

Then we obtain the main result of [4] as follows.

THEOREM 5.2. *Let L be a hyperbolic link with a fixed diagram and $V(z_1, \dots, z_g)$ be the potential function of the diagram. Assume that the solution set $\mathcal{S} = \cup_{j \in J'} \mathcal{S}_j$ is not empty. Then, for any $\mathbf{z} \in \mathcal{S}_j$, $V_0(\mathbf{z})$ is constant (it depends only on j) and*

$$V_0(\mathbf{z}) \equiv i(\text{vol}(\rho_{\mathbf{z}}) + i \text{cs}(\rho_{\mathbf{z}})) \text{ mod } \pi^2,$$

where $\rho_{\mathbf{z}}$ is the boundary-parabolic representation in (5.2). Furthermore, there exists a path component \mathcal{S}_0 of \mathcal{S} satisfying

$$V_0(\mathbf{z}_{\infty}) \equiv i(\text{vol}(L) + i \text{cs}(L)) \text{ mod } \pi^2$$

for all $\mathbf{z}_{\infty} \in \mathcal{S}_0$.

We call the value $V_0(\mathbf{z})$ the optimistic limit of the Kashaev invariant. Note that it depends on the choice of the diagram and the path component \mathcal{S}_j .

6. Proof of Theorem 1.3

This section is devoted to the proof of Theorem 1.3. Note that it was almost proved in [6], so we will skip several calculations and refer to the results in [6].

To avoid redundant calculations, we change the definition of W_N in Figure 3 to that below:

$$\begin{aligned}
 W_N := & \operatorname{Li}_2\left(\frac{w_l}{w_m}\right) + \operatorname{Li}_2\left(\frac{w_l}{w_k}\right) - \operatorname{Li}_2\left(\frac{w_j w_l}{w_k w_m}\right) \\
 & - \operatorname{Li}_2\left(\frac{w_m}{w_j}\right) - \operatorname{Li}_2\left(\frac{w_k}{w_j}\right) + \frac{\pi^2}{6} - \log \frac{w_j}{w_m} \log \frac{w_j}{w_k}.
 \end{aligned}
 \tag{6.1}$$

It is possible because, by using \approx to denote the equivalence relation defined in [6, Lemma 3.1], we know that

$$\log \frac{w_j}{w_m} \log \frac{w_j}{w_k} \approx (\log w_j - \log w_m)(\log w_j - \log w_k) \approx \log \frac{w_m}{w_j} \log \frac{w_k}{w_j}.$$

Therefore, changing $\log(w_m/w_j) \log(w_k/w_j)$ of W_N to $\log(w_j/w_m) \log(w_j/w_k)$ does not have any effect on \mathcal{I} and the optimistic limit $W_0(\mathbf{w})$.

LEMMA 6.1. Fix an oriented diagram D of the hyperbolic link L , which does not have a kink. For a solution $\mathbf{w} = (w_1, \dots, w_n) \in \mathcal{T}$, if the variables w_j, \dots, w_m in Figure 1 satisfy

$$w_j + w_l \neq w_k + w_m
 \tag{6.2}$$

at all crossings, then there exists a solution $\mathbf{z} \in \mathcal{S}$ satisfying $\rho_{\mathbf{w}} = \rho_{\mathbf{z}}$. Inversely, for a solution $\mathbf{z} = (z_1, \dots, z_g) \in \mathcal{S}$, there always exists a solution $\mathbf{w} \in \mathcal{T}$ satisfying $\rho_{\mathbf{z}} = \rho_{\mathbf{w}}$.

PROOF. For a hyperbolic ideal octahedron in Figure 15, we assign shape parameters $t_1, t_2, t_3, t_4, u_1, u_2, u_3$ and u_4 to the edges CD, DA, AB, BC, CF, DE, AF and BE, respectively. Let $u_5 := 1/(u_1 u_3) = 1/(u_2 u_4)$ be the shape parameter of the tetrahedron ABCD assigned to the edges AC and BD.

Then we obtain the following relations.

$$\begin{cases} t_1 = u'_1 u''_2 u'_5, \\ t_2 = u'_2 u'_3 u''_5, \\ t_3 = u''_3 u'_4 u'_5, \\ t_4 = u'_4 u'_1 u''_5, \end{cases} \quad \begin{cases} u_1 = t'_1 t''_4, \\ u_2 = t'_1 t'_2, \\ u_3 = t'_3 t'_2, \\ u_4 = t'_3 t'_4, \\ u_5 = (t'_1 t''_2 t'_3 t'_4)^{-1}. \end{cases}
 \tag{6.3}$$

Now we consider the octahedra placed on the crossings in Figure 7. Note that the five-term triangulation and the four-term triangulation use the same octahedral

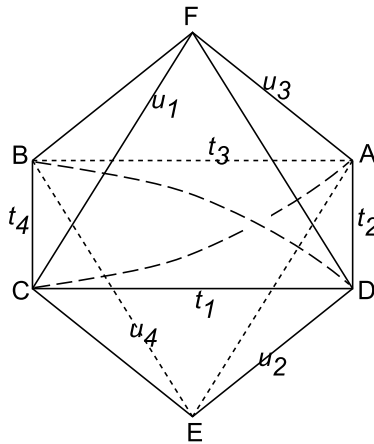


FIGURE 15. Assignment of variables.

decomposition of $\mathbb{S}^3 \setminus (L \cup \{\pm\infty\})$, but the subdividing methods are different. Therefore, if we apply (6.3) to the octahedral decomposition, we can find relations between variables w_1, \dots, w_n and z_1, \dots, z_g . The octahedron in Figure 1(a) (or the one in Figure 7(a)) gives the relations

$$\begin{cases} \frac{z_b}{z_a} = \left(\frac{w_m}{w_j}\right)'' \left(\frac{w_k}{w_j}\right)'' \left(\frac{w_j w_l}{w_k w_m}\right)', & \frac{z_c}{z_b} = \left(\frac{w_k}{w_j}\right)' \left(\frac{w_l}{w_l}\right)' \left(\frac{w_j w_l}{w_k w_m}\right)'', \\ \frac{z_d}{z_c} = \left(\frac{w_k}{w_l}\right)'' \left(\frac{w_m}{w_l}\right)'' \left(\frac{w_j w_l}{w_k w_m}\right)', & \frac{z_a}{z_d} = \left(\frac{w_m}{w_l}\right)' \left(\frac{w_m}{w_j}\right)' \left(\frac{w_j w_l}{w_k w_m}\right)''. \end{cases} \tag{6.4}$$

and

$$\begin{cases} \frac{w_m}{w_j} = \left(\frac{z_b}{z_a}\right)' \left(\frac{z_a}{z_d}\right)'', & \frac{w_k}{w_j} = \left(\frac{z_b}{z_a}\right)' \left(\frac{z_c}{z_b}\right)'', & \frac{w_l}{w_l} = \left(\frac{z_d}{z_c}\right)' \left(\frac{z_c}{z_b}\right)'', \\ \frac{w_m}{w_l} = \left(\frac{z_d}{z_c}\right)' \left(\frac{z_a}{z_d}\right)'', & \frac{w_j w_l}{w_k w_m} = \left(\frac{z_a}{z_b}\right)'' \left(\frac{z_b}{z_c}\right)' \left(\frac{z_c}{z_d}\right)'' \left(\frac{z_d}{z_a}\right)'. \end{cases} \tag{6.5}$$

The octahedron in Figure 1(b) (or the one in Figure 7(b)) gives the relations

$$\begin{cases} \frac{z_b}{z_a} = \left(\frac{w_j}{w_m}\right)' \left(\frac{w_j}{w_k}\right)' \left(\frac{w_k w_m}{w_j w_l}\right)'', & \frac{z_c}{z_b} = \left(\frac{w_j}{w_k}\right)'' \left(\frac{w_l}{w_k}\right)'' \left(\frac{w_k w_m}{w_j w_l}\right)', \\ \frac{z_d}{z_c} = \left(\frac{w_l}{w_k}\right)' \left(\frac{w_l}{w_m}\right)' \left(\frac{w_k w_m}{w_j w_l}\right)'', & \frac{z_a}{z_d} = \left(\frac{w_l}{w_m}\right)'' \left(\frac{w_j}{w_m}\right)'' \left(\frac{w_k w_m}{w_j w_l}\right)'. \end{cases} \tag{6.6}$$

and

$$\begin{cases} \frac{w_j}{w_m} = \left(\frac{z_a}{z_d}\right)' \left(\frac{z_b}{z_a}\right)'', & \frac{w_j}{w_k} = \left(\frac{z_c}{z_b}\right)' \left(\frac{z_b}{z_a}\right)'', & \frac{w_l}{w_k} = \left(\frac{z_c}{z_b}\right)' \left(\frac{z_d}{z_c}\right)'', \\ \frac{w_l}{w_m} = \left(\frac{z_a}{z_d}\right)' \left(\frac{z_d}{z_c}\right)'', & \frac{w_k w_m}{w_j w_l} = \left(\frac{z_a}{z_b}\right)' \left(\frac{z_b}{z_c}\right)'' \left(\frac{z_c}{z_d}\right)' \left(\frac{z_d}{z_a}\right)''. \end{cases} \tag{6.7}$$

If w_j, \dots, w_m of each crossing is fixed, then we can determine z_a, \dots, z_d using (6.5) and (6.7), and the inverse can be done using (6.4) and (6.6). Furthermore, if we consider $\mathbf{w} \in \mathbb{C}\mathbb{P}^{m-1}$ and $\mathbf{z} \in \mathbb{C}\mathbb{P}^{g-1}$, then \mathbf{w} determines \mathbf{z} uniquely and vice versa.

For the set of equations

$$\begin{cases} \left(\frac{w_m}{w_j}\right)'' \left(\frac{w_k}{w_j}\right)'' \left(\frac{w_j w_l}{w_k w_m}\right)' \neq 1, & \left(\frac{w_k}{w_j}\right)' \left(\frac{w_k}{w_l}\right)' \left(\frac{w_j w_l}{w_k w_m}\right)'' \neq 1, \\ \left(\frac{w_k}{w_l}\right)'' \left(\frac{w_m}{w_l}\right)'' \left(\frac{w_j w_l}{w_k w_m}\right)' \neq 1, & \left(\frac{w_m}{w_l}\right)' \left(\frac{w_m}{w_j}\right)' \left(\frac{w_j w_l}{w_k w_m}\right)'' \neq 1 \end{cases} \tag{6.8}$$

in (6.4) and

$$\begin{cases} \left(\frac{w_j}{w_m}\right)' \left(\frac{w_j}{w_k}\right)' \left(\frac{w_k w_m}{w_j w_l}\right)'' \neq 1, & \left(\frac{w_j}{w_k}\right)'' \left(\frac{w_l}{w_k}\right)'' \left(\frac{w_k w_m}{w_j w_l}\right)' \neq 1, \\ \left(\frac{w_l}{w_k}\right)' \left(\frac{w_l}{w_m}\right)' \left(\frac{w_k w_m}{w_j w_l}\right)'' \neq 1, & \left(\frac{w_l}{w_m}\right)'' \left(\frac{w_j}{w_m}\right)'' \left(\frac{w_k w_m}{w_j w_l}\right)' \neq 1 \end{cases} \tag{6.9}$$

in (6.6), direct calculation shows that (6.8), (6.9) and (6.2) are equivalent to each other. Therefore, (6.2) guarantees that \mathbf{z} determines a solution for $\mathbf{z} \in \mathcal{S}$.

Also, for the set of equations

$$\begin{cases} \left(\frac{z_b}{z_a}\right)' \left(\frac{z_a}{z_d}\right)'' \neq 1, & \left(\frac{z_b}{z_a}\right)' \left(\frac{z_c}{z_b}\right)'' \neq 1, & \left(\frac{z_d}{z_c}\right)' \left(\frac{z_c}{z_b}\right)'' \neq 1, \\ \left(\frac{z_d}{z_c}\right)' \left(\frac{z_a}{z_d}\right)'' \neq 1, & \left(\frac{z_a}{z_b}\right)'' \left(\frac{z_b}{z_c}\right)' \left(\frac{z_c}{z_d}\right)'' \left(\frac{z_d}{z_a}\right)' \neq 1 \end{cases} \tag{6.10}$$

in (6.5) and

$$\begin{cases} \left(\frac{z_a}{z_d}\right)' \left(\frac{z_b}{z_a}\right)'' \neq 1, & \left(\frac{z_c}{z_b}\right)' \left(\frac{z_b}{z_a}\right)'' \neq 1, & \left(\frac{z_c}{z_b}\right)' \left(\frac{z_d}{z_c}\right)'' \neq 1, \\ \left(\frac{z_a}{z_d}\right)' \left(\frac{z_d}{z_c}\right)'' \neq 1, & \left(\frac{z_a}{z_b}\right)' \left(\frac{z_b}{z_c}\right)'' \left(\frac{z_c}{z_d}\right)' \left(\frac{z_d}{z_a}\right)'' \neq 1 \end{cases} \tag{6.11}$$

in (6.7), direct calculation shows that (6.10), (6.11) and $z_a \neq z_c, z_b \neq z_d$ are equivalent to each other. The latter is the assumption of the solution; hence, any $\mathbf{z} \in \mathcal{S}$ determines a solution $\mathbf{w} \in \mathcal{T}$.

Finally, if \mathbf{z} and \mathbf{w} are related as above, then they determine the same octahedral decomposition and the same developing map. Therefore, we conclude that $\rho_{\mathbf{z}} = \rho_{\mathbf{w}}$. \square

Let $D(z) := \text{Im Li}_2(z) + \log |z| \arg(1 - z)$ be the Bloch–Wigner function for $z \in \mathbb{C} \setminus \{0, 1\}$. It is a well-known fact that $D(z) = \text{vol}(T_z)$, where T_z is the hyperbolic ideal tetrahedron with the shape parameter z . Therefore, from Figure 15,

$$D(t_1) + D(t_2) + D(t_3) + D(t_4) = D(u_1) + D(u_2) + D(u_3) + D(u_4) + D(u_5). \tag{6.12}$$

Note that the variables $t_1, \dots, t_4, u_1, \dots, u_5$ satisfying (6.3) determine a hyperbolic ideal octahedron in Figure 15, so (6.3) guarantees (6.12).

LEMMA 6.2. *Let $t_1, t_2, t_3, t_4, u_1, u_2, u_3, u_4, u_5 \notin \{0, 1, \infty\}$ be the shape parameters defined in the hyperbolic octahedron in Figure 15, which satisfies (6.3) and (6.12). Then the following identities hold for any choice of log-branch modulo $4\pi^2$.*

$$\begin{aligned}
 & \operatorname{Li}_2(t_1) - \operatorname{Li}_2\left(\frac{1}{t_2}\right) + \operatorname{Li}_2(t_3) - \operatorname{Li}_2\left(\frac{1}{t_4}\right) \\
 & \equiv \operatorname{Li}_2(u_1) + \operatorname{Li}_2(u_2) - \operatorname{Li}_2\left(\frac{1}{u_3}\right) - \operatorname{Li}_2\left(\frac{1}{u_4}\right) + \operatorname{Li}_2(u_5) - \frac{\pi^2}{6} + \log u_1 \log u_2 \\
 & \quad - \left(-\log(1 - t_1) + \log\left(1 - \frac{1}{t_4}\right)\right) \log u_2 \\
 & \quad - \left(-\log(1 - t_1) + \log\left(1 - \frac{1}{t_2}\right)\right) \log u_1 \\
 & \quad + \left(-\log(1 - t_1) + \log\left(1 - \frac{1}{t_4}\right)\right) \log(1 - u_1) \\
 & \quad + \left(-\log(1 - t_1) + \log\left(1 - \frac{1}{t_2}\right)\right) \log(1 - u_2) \\
 & \quad + \left(-\log(1 - t_3) + \log\left(1 - \frac{1}{t_2}\right)\right) \log\left(1 - \frac{1}{u_3}\right) \\
 & \quad + \left(-\log(1 - t_3) + \log\left(1 - \frac{1}{t_4}\right)\right) \log\left(1 - \frac{1}{u_4}\right) \\
 & \quad + \left(\log(1 - t_1) - \log\left(1 - \frac{1}{t_2}\right) + \log(1 - t_3) - \log\left(1 - \frac{1}{t_4}\right)\right) \log(1 - u_5) \\
 & \equiv \operatorname{Li}_2(u_1) - \operatorname{Li}_2\left(\frac{1}{u_2}\right) - \operatorname{Li}_2\left(\frac{1}{u_3}\right) + \operatorname{Li}_2(u_4) - \operatorname{Li}_2\left(\frac{1}{u_5}\right) + \frac{\pi^2}{6} - \log u_2 \log u_3 \\
 & \quad + \left(-\log(1 - t_3) + \log\left(1 - \frac{1}{t_2}\right)\right) \log u_2 \\
 & \quad + \left(-\log(1 - t_1) + \log\left(1 - \frac{1}{t_2}\right)\right) \log u_3 \\
 & \quad + \left(-\log(1 - t_1) + \log\left(1 - \frac{1}{t_4}\right)\right) \log(1 - u_1) \\
 & \quad + \left(-\log(1 - t_1) + \log\left(1 - \frac{1}{t_2}\right)\right) \log\left(1 - \frac{1}{u_2}\right) \\
 & \quad + \left(-\log(1 - t_3) + \log\left(1 - \frac{1}{t_2}\right)\right) \log\left(1 - \frac{1}{u_3}\right) \\
 & \quad + \left(-\log(1 - t_3) + \log\left(1 - \frac{1}{t_4}\right)\right) \log(1 - u_4) \\
 & \quad + \left(\log(1 - t_1) - \log\left(1 - \frac{1}{t_2}\right) + \log(1 - t_3) - \log\left(1 - \frac{1}{t_4}\right)\right) \log\left(1 - \frac{1}{u_5}\right) \\
 & \text{mod } 4\pi^2.
 \end{aligned}$$

PROOF. See the proof of [6, Lemma 5.1]. □

Let $\mathbf{w} \in \mathcal{T}$ and $\mathbf{z} \in \mathcal{S}$ be the corresponding pair in Lemma 6.1. To prove

$$V_0(\mathbf{z}) \equiv W_0(\mathbf{w}) \pmod{4\pi^2}, \tag{6.13}$$

we consider the two cases of the crossing with parameters $z_a, \dots, z_d, w_j, \dots, w_m$ in Figure 1.

For the case of Figure 1(a), we let $t_1 = z_b/z_a, t_2 = z_c/z_b, t_3 = z_d/z_c, t_4 = z_a/z_d, u_1 = w_m/w_j, u_2 = w_k/w_j, u_3 = w_k/w_l, u_4 = w_m/w_l$ and $u_5 = (w_j w_l)/(w_k w_m)$, so that (6.3) is satisfied. Then the potential function of a crossing defined in Figure 12 is expressed by

$$V_P(z_a, \dots, z_d) := \text{Li}_2(t_1) - \text{Li}_2\left(\frac{1}{t_2}\right) + \text{Li}_2(t_3) - \text{Li}_2\left(\frac{1}{t_4}\right)$$

and the potential function of a positive crossing defined in Figure 3(a) is expressed by

$$\begin{aligned} &W_P(w_j, w_k, w_l, w_m) \\ &= \text{Li}_2(u_1) + \text{Li}_2(u_2) - \text{Li}_2\left(\frac{1}{u_3}\right) - \text{Li}_2\left(\frac{1}{u_4}\right) + \text{Li}_2(u_5) - \frac{\pi^2}{6} + \log u_1 \log u_2. \end{aligned}$$

Using Lemma 6.2, we can calculate

$$\begin{aligned} V_{P0} - W_{P0} &\equiv -(\log w_j - \log w_m) \log z_a - (\log w_k - \log w_j) \log z_b \\ &\quad + (\log w_k - \log w_l) \log z_c \\ &\quad + (\log w_l - \log w_m) \log z_d \pmod{4\pi^2}. \end{aligned} \tag{6.14}$$

(The detailed calculations are in [6, (41)–(42)] and the following paragraphs. Note that, in [6], we denoted V_P and W_P by $X(z_a, \dots, z_d)$ and $P_1(w_j, \dots, w_m)$, respectively.)

For the case of Figure 1(b), we let $t_1 = z_a/z_d, t_2 = z_b/z_a, t_3 = z_c/z_b, t_4 = z_d/z_c, u_1 = w_l/w_m, u_2 = w_j/w_m, u_3 = w_j/w_k, u_4 = w_l/w_k$ and $u_5 = (w_k w_m)/(w_j w_l)$, so that (6.3) is satisfied. Then the potential function of a crossing defined in Figure 12 is expressed by

$$V_N(z_a, \dots, z_d) := \text{Li}_2(t_1) - \text{Li}_2\left(\frac{1}{t_2}\right) + \text{Li}_2(t_3) - \text{Li}_2\left(\frac{1}{t_4}\right)$$

and the potential function of a negative crossing defined in (6.1) is expressed by

$$\begin{aligned} &W_N(w_j, w_k, w_l, w_m) \\ &= \text{Li}_2(u_1) - \text{Li}_2\left(\frac{1}{u_2}\right) - \text{Li}_2\left(\frac{1}{u_3}\right) + \text{Li}_2(u_4) - \text{Li}_2\left(\frac{1}{u_5}\right) + \frac{\pi^2}{6} - \log u_2 \log u_3. \end{aligned}$$

Using Lemma 6.2, we can calculate

$$\begin{aligned} V_{N0} - W_{N0} &\equiv -(\log w_j - \log w_m) \log z_a - (\log w_k - \log w_j) \log z_b \\ &\quad + (\log w_k - \log w_l) \log z_c \\ &\quad + (\log w_l - \log w_m) \log z_d \pmod{4\pi^2}. \end{aligned} \tag{6.15}$$

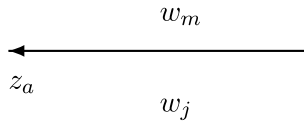


FIGURE 16. Side assigned by z_a .

Note that the right-hand sides of (6.14) and (6.15) coincide. We can deduce the general rule of these equations using Figure 16.

For the side with z_a in Figure 16, when it goes out of a crossing, the contribution to (6.14) or (6.15) of the crossing is

$$-(\log w_j - \log w_m) \log z_a$$

and, when it goes into a crossing, the contribution is

$$+(\log w_j - \log w_m) \log z_a.$$

Therefore, if we consider the whole crossings of the link diagram, the right-hand sides of (6.14) or (6.15) at all crossings are cancelled out and we obtain (6.13). This completes the proof of Theorem 1.3.

7. Example of the twist knots

In this section, we apply Theorem 1.3 to the example of the twist knot in [4, Section 6] and show several numerical results. For the calculations, we assume the principal branch of logarithm. Also, we use the definition of W_N in Figure 3(b).

Let T_n ($n \geq 1$) be the twist knot with $n + 3$ crossings in Figure 17. For example, T_1 is the figure-eight knot 4_1 and T_2 is the 5_2 knot. We follow the orientations in Figure 17.

We assign variables $a, b, x_0, \dots, x_{n+1}, y_0, \dots, y_{n+1}$ to the sides and $c, d, e, w_0, \dots, w_{n+1}$ to the regions of Figure 17, respectively. Let

$$\begin{aligned}
 A_k &:= \text{Li}_2\left(\frac{c}{w_k}\right) + \text{Li}_2\left(\frac{c}{w_{k+1}}\right) - \text{Li}_2\left(\frac{ce}{w_k w_{k+1}}\right) - \text{Li}_2\left(\frac{w_k}{e}\right) - \text{Li}_2\left(\frac{w_{k+1}}{e}\right) \\
 &\quad + \frac{\pi^2}{6} - \log \frac{w_k}{e} \log \frac{w_{k+1}}{e}, \\
 B_k &:= \text{Li}_2\left(\frac{e}{w_k}\right) + \text{Li}_2\left(\frac{e}{w_{k+1}}\right) - \text{Li}_2\left(\frac{ce}{w_k w_{k+1}}\right) - \text{Li}_2\left(\frac{w_k}{c}\right) - \text{Li}_2\left(\frac{w_{k+1}}{c}\right) \\
 &\quad + \frac{\pi^2}{6} - \log \frac{w_k}{c} \log \frac{w_{k+1}}{c}
 \end{aligned}$$

for $k = 0, 1, \dots, n$. If n is odd, the potential function $W(T_n; c, d, e, w_0, \dots, w_{n+1})$ of Figure 17(a) is

$$\begin{aligned}
 &W(T_n; c, d, e, w_0, \dots, w_{n+1}) \\
 &= \left\{ -\text{Li}_2\left(\frac{w_{n+1}}{c}\right) - \text{Li}_2\left(\frac{w_{n+1}}{d}\right) + \text{Li}_2\left(\frac{w_0 w_{n+1}}{cd}\right) + \text{Li}_2\left(\frac{c}{w_0}\right) + \text{Li}_2\left(\frac{d}{w_0}\right) \right\}
 \end{aligned}$$

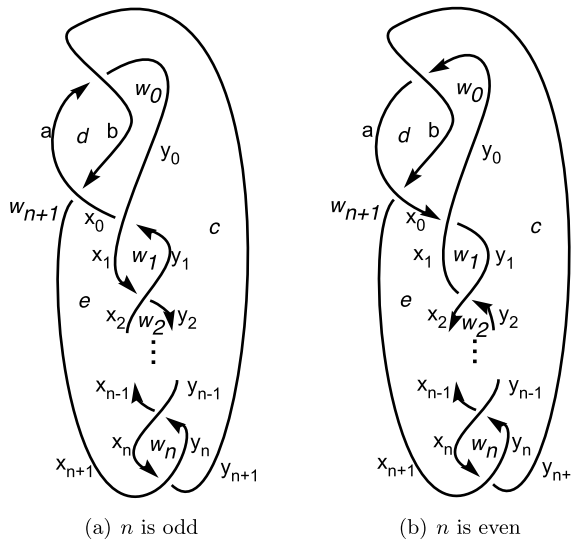


FIGURE 17. Twist knot T_n .

$$\begin{aligned}
 & \left. -\frac{\pi^2}{6} + \log \frac{c}{w_0} \log \frac{d}{w_0} \right\} \\
 & + \left\{ -\text{Li}_2\left(\frac{w_0}{d}\right) - \text{Li}_2\left(\frac{w_0}{e}\right) + \text{Li}_2\left(\frac{w_0 w_{n+1}}{de}\right) + \text{Li}_2\left(\frac{d}{w_{n+1}}\right) + \text{Li}_2\left(\frac{e}{w_{n+1}}\right) \right. \\
 & \left. -\frac{\pi^2}{6} + \log \frac{d}{w_{n+1}} \log \frac{e}{w_{n+1}} \right\} \\
 & + \sum_{k=0}^{(n-1)/2} (A_{2k} + B_{2k+1})
 \end{aligned}$$

and, if n is even, the potential function $W(T_n; c, d, e, w_0, \dots, w_{n+1})$ of Figure 17(b) is

$$\begin{aligned}
 & W(T_n; c, d, e, w_0, \dots, w_{n+1}) \\
 & = \left\{ \text{Li}_2\left(\frac{c}{w_0}\right) + \text{Li}_2\left(\frac{c}{w_{n+1}}\right) - \text{Li}_2\left(\frac{cd}{w_0 w_{n+1}}\right) - \text{Li}_2\left(\frac{w_0}{d}\right) - \text{Li}_2\left(\frac{w_{n+1}}{d}\right) \right. \\
 & \quad \left. + \frac{\pi^2}{6} - \log \frac{w_0}{d} \log \frac{w_{n+1}}{d} \right\} \\
 & + \left\{ \text{Li}_2\left(\frac{d}{w_0}\right) + \text{Li}_2\left(\frac{d}{w_{n+1}}\right) - \text{Li}_2\left(\frac{de}{w_0 w_{n+1}}\right) - \text{Li}_2\left(\frac{w_0}{e}\right) - \text{Li}_2\left(\frac{w_{n+1}}{e}\right) \right. \\
 & \quad \left. + \frac{\pi^2}{6} - \log \frac{w_0}{e} \log \frac{w_{n+1}}{e} \right\} \\
 & + B_0 + \sum_{k=1}^{n/2} (A_{2k-1} + B_{2k}).
 \end{aligned}$$

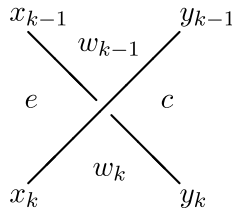


FIGURE 18. The $(k + 2)$ th crossing for $k = 1, \dots, n + 1$.

TABLE 1. Defining equation of t for $n = 1, \dots, 5$.

n	Defining equation of t
1	$16 - 12t + 3t^2 = 0$
2	$-64 + 80t - 40t^2 + 7t^3 = 0$
3	$256 - 448t + 336t^2 - 120t^3 + 17t^4 = 0$
4	$-2048 + 4608t - 4608t^2 + 2464t^3 - 696t^4 + 82t^5 = 0$
5	$4096 - 11264t + 14080t^2 - 9984t^3 + 4192t^4 - 980t^5 + 99t^6 = 0$

In [4, Section 6], we chose $(a, b, x_0, \dots, x_{n+1}, y_0, \dots, y_{n+1})$ by

$$a = 2, \quad b = -1, \quad x_0 = t, \quad y_0 = 1 + \frac{2}{t}, \quad x_1 = \frac{t(t + 2)}{t^2 - 4t + 8}, \quad y_1 = \frac{4}{t},$$

$$x_{k+1} = \frac{x_k y_k}{-x_{k-1} + x_k + y_k}, \quad y_{k+1} = x_k + y_k - \frac{x_k y_k}{y_{k-1}}, \quad x_{n+1} = 3, \quad y_{n+1} = 1,$$

where $k = 1, \dots, n - 1$ and t is a solution of the defining equation in Table 1. All the solutions t of the defining equation determine the solutions in \mathcal{S} and the corresponding representation

$$\rho(T_n)(t) : \pi_1(\mathbb{S}^3 \setminus T_n) \longrightarrow \text{PSL}(2, \mathbb{C}).$$

Using the equations (6.5) and (6.7), we can express $(c, d, e, w_0, \dots, w_{n+1})$ in terms of t . Specifically, the $(k + 2)$ th crossing (in the order from top to bottom) in Figure 17 becomes Figure 18 and it determines

$$\frac{e}{w_k} = \left(\frac{y_k}{x_k}\right)' \left(\frac{x_k}{x_{k-1}}\right)''$$

for $k = 1, \dots, n + 1$. The first crossing in Figure 17 gives an equation of c :

$$\frac{c}{w_{n+1}} = \left(\frac{a}{y_{n+1}}\right)' \left(\frac{y_{n+1}}{y_0}\right)'' = \frac{2}{t}.$$

The second crossing in Figure 17 gives a more simple equation of w_{n+1} :

$$\frac{e}{w_{n+1}} = \left(\frac{x_{n+1}}{a}\right)' \left(\frac{x_0}{x_{n+1}}\right)'' = -\frac{2(t - 3)}{t}$$

and other equations of d and w_0 :

$$\frac{d}{w_{n+1}} = \left(\frac{x_{n+1}}{a}\right)' \left(\frac{a}{b}\right)'' = -3, \quad \frac{e}{w_0} = \left(\frac{b}{x_0}\right)' \left(\frac{x_0}{x_{n+1}}\right)'' = \frac{t - 3}{t + 1}.$$

TABLE 2. Expressions of w_k in terms of t for $k = 0, \dots, 6$.

k	w_k
0	$(1 + t)/(-3 + t)$
1	$-(16 + t^2)/((-3 + t)t^2)$
2	$(256 - 256t + 112t^2 - 16t^3 - 3t^4 + t^5)/((-3 + t)t^4)$
3	$(-4096 + 8192t - 7424t^2 + 3584t^3 - 864t^4 + 32t^5 + 27t^6 - 4t^7)/((-3 + t)t^6)$
4	$(65536 - 196608t + 274432t^2 - 225280t^3 + 115456t^4 - 35584t^5 + 5152t^6 + 320t^7 - 231t^8 + 25t^9)/((-3 + t)t^8)$
5	$(-1048576 + 4194304t - 7929856t^2 + 9175040t^3 - 7094272t^4 + 3760128t^5 - 1337088t^6 + 287232t^7 - 21232t^8 - 6048t^9 + 1751t^{10} - 144t^{11})/((-3 + t)t^{10})$
6	$(16777216 - 83886080t + 200278016t^2 - 298844160t^3 + 307822592t^4 - 228524032t^5 + 123846656t^6 - 48324608t^7 + 12842496t^8 - 1930752t^9 - 2544t^{10} + 66288t^{11} - 12587t^{12} + 841t^{13})/((-3 + t)t^{12})$

Therefore, after choosing $e = 1$, we can express $(c, d, e, w_0, \dots, w_{n+1})$ in terms of t by

$$c = -\frac{1}{t-3}, \quad d = \frac{3t}{2(t-3)}, \quad e = 1, \quad w_0 = \frac{t+1}{t-3}, \quad w_k = \left(\frac{x_k}{y_k}\right)'' \left(\frac{x_{k-1}}{x_k}\right)'$$

for $k = 1, \dots, n + 1$. The exact expression of w_k for $k = 1, \dots, 6$ is in Table 2.

For the solutions t of the defining equations, the numerical values of the corresponding optimistic limits

$$W_0(T_n)(t) \equiv i(\text{vol}(\rho(T_n)(t)) + i \text{cs}(\rho(T_n)(t))) \text{ mod } \pi^2$$

for $n = 1, \dots, 5$ are in Table 3. Note that these values exactly coincide with the optimistic limits of Kashaev invariants in [4, Table 3].

Appendix A. Change of the signs of the variables

In this appendix, we show that the change of the signs of the variables of the potential function does not have an effect on the set of equations \mathcal{I} and the optimistic limit. Note that this property will be used in the author’s later article.

Let $W(w_1, \dots, w_n)$ be the potential function defined in Section 2. Let $\tau_1, \dots, \tau_n, \epsilon_1, \dots, \epsilon_n \in \{-1, 1\}$ be fixed signs and define another potential function

$$\widetilde{W}(w_1, \dots, w_n) := W(\tau_1 w_1^{\epsilon_1}, \dots, \tau_n w_n^{\epsilon_n}).$$

In the same way, we define

$$\widetilde{\mathcal{I}} := \left\{ \exp\left(w_k \frac{\partial \widetilde{W}}{\partial w_k}\right) = 1 \mid k = 1, \dots, n \right\}$$

and let $\widetilde{\mathcal{T}}$ be the solution set of $\widetilde{\mathcal{I}}$. Also, for $\mathbf{w} = (w_1, \dots, w_n)$, define

$$\widetilde{\mathbf{w}} := (\tau_1 w_1^{\epsilon_1}, \dots, \tau_n w_n^{\epsilon_n}).$$

TABLE 3. Values of $W_0(T_n)(t)$ for $n = 1, \dots, 5$.

n	t	$W_0(T_n)(t)$
1	$t = 2 + 1.1547 \dots i$	$i(2.0299 \dots + 0i)$
	$t = 2 - 1.1547 \dots i$	$i(-2.0299 \dots + 0i)$
2	$t = 1.4587 \dots + 1.0682 \dots i$	$i(2.8281 \dots + 3.0241 \dots i)$
	$t = 1.4587 \dots - 1.0682 \dots i$	$i(-2.8281 \dots + 3.0241 \dots i)$
	$t = 2.7969 \dots$	$i(0 - 1.1135 \dots i)$
3	$t = 1.2631 \dots + 1.0347 \dots i$	$i(3.1640 \dots + 6.7907 \dots i)$
	$t = 1.2631 \dots - 1.0347 \dots i$	$i(-3.1640 \dots + 6.7907 \dots i)$
	$t = 2.2664 \dots + 0.7158 \dots i$	$i(1.4151 \dots + 0.2110 \dots i)$
	$t = 2.2664 \dots - 0.7158 \dots i$	$i(-1.4151 \dots + 0.2110 \dots i)$
4	$t = 1.1713 \dots + 1.0202 \dots i$	$i(3.3317 \dots + 10.9583 \dots i)$
	$t = 1.1713 \dots - 1.0202 \dots i$	$i(-3.3317 \dots + 10.9583 \dots i)$
	$t = 1.8097 \dots + 0.9073 \dots i$	$i(2.2140 \dots + 1.8198 \dots i)$
	$t = 1.8097 \dots - 0.9073 \dots i$	$i(-2.2140 \dots + 1.8198 \dots i)$
	$t = 2.5257 \dots$	$i(0 - 0.8822 \dots i)$
5	$t = 1.1208 \dots + 1.0129 \dots i$	$i(3.4272 \dots + 15.3545 \dots i)$
	$t = 1.1208 \dots - 1.0129 \dots i$	$i(-3.4272 \dots + 15.3545 \dots i)$
	$t = 1.5498 \dots + 0.9676 \dots i$	$i(2.6560 \dots + 4.6428 \dots i)$
	$t = 1.5498 \dots - 0.9676 \dots i$	$i(-2.6560 \dots + 4.6428 \dots i)$
	$t = 2.2789 \dots + 0.4876 \dots i$	$i(1.1087 \dots - 0.2581 \dots i)$
	$t = 2.2789 \dots - 0.4876 \dots i$	$i(-1.1087 \dots - 0.2581 \dots i)$

PROPOSITION A.1. *There is a one-to-one correspondence between $\mathbf{w} \in \mathcal{T}$ and $\tilde{\mathbf{w}} \in \tilde{\mathcal{T}}$. Furthermore,*

$$\tilde{W}_0(\tilde{\mathbf{w}}) \equiv W_0(\mathbf{w}) \pmod{2\pi^2}. \tag{A.1}$$

PROOF. At first, we show that $\tilde{\mathbf{w}} \in \tilde{\mathcal{T}}$ for each $\mathbf{w} \in \mathcal{T}$. Note that

$$w_k \frac{\partial}{\partial w_k} \text{Li}_2\left(\frac{\tau_k w_k^{\epsilon_k}}{\tau_j w_j^{\epsilon_j}}\right) = \epsilon_k \cdot \log\left(1 - \frac{\tau_k w_k^{\epsilon_k}}{\tau_j w_j^{\epsilon_j}}\right)$$

implies that

$$w_k \frac{\partial}{\partial w_k} \text{Li}_2\left(\frac{\tau_k w_k^{\epsilon_k}}{\tau_j w_j^{\epsilon_j}}\right) \Big|_{\mathbf{w}=\tilde{\mathbf{w}}} = \epsilon_k \cdot \log\left(1 - \frac{w_k}{w_j}\right) = \epsilon_k \cdot w_k \frac{\partial}{\partial w_k} \text{Li}_2\left(\frac{w_k}{w_j}\right),$$

where $|_{\mathbf{w}=\tilde{\mathbf{w}}}$ means the evaluation of the equation at $\tilde{\mathbf{w}}$. Therefore,

$$w_k \frac{\partial \tilde{W}}{\partial w_k} \Big|_{\mathbf{w}=\tilde{\mathbf{w}}} = \epsilon_k \cdot w_k \frac{\partial W}{\partial w_k}, \tag{A.2}$$

which shows that $\tilde{\mathbf{w}} \in \tilde{\mathcal{T}}$ and the coincidence of \mathcal{I} and $\tilde{\mathcal{I}}$. Therefore, there is a one-to-one correspondence between \mathcal{T} and $\tilde{\mathcal{T}}$.

Note that $\tilde{W}(\tilde{\mathbf{w}}) = W(\mathbf{w})$ holds trivially. For $\mathbf{w} \in \mathcal{T}$, the value of (A.2) is zero modulo $2\pi i$. Therefore, (A.1) follows from

$$\left(w_k \frac{\partial \tilde{W}}{\partial w_k}\right) \log w_k \Big|_{\mathbf{w}=\tilde{\mathbf{w}}} \equiv \epsilon_k \cdot \left(w_k \frac{\partial W}{\partial w_k}\right) \log(\tau_k w_k^{\epsilon_k}) \equiv \left(w_k \frac{\partial W}{\partial w_k}\right) \log w_k \pmod{2\pi^2}. \quad \square$$

We finally remark that the same result holds for the potential function of the Kashaev invariant in Section 5 by exactly the same arguments.

Acknowledgements

The author appreciates Jun Murakami, Yuichi Kabaya, Hyuk Kim and Seonhwa Kim for discussions and suggestions on this work. He also appreciates the referee for suggesting many important improvements.

References

- [1] J. Cho, ‘Optimistic limit of the colored Jones polynomial and the existence of a solution’, *Proc. Amer. Math. Soc.* **144** (2016), 1803–1814.
- [2] J. Cho, Quandle theory and optimistic limits of representations of knot groups. Preprint, 2014, [arXiv:1409.1764](https://arxiv.org/abs/1409.1764).
- [3] J. Cho, ‘Connected sum of representations of knot groups’, *J. Knot Theory Ramifications* **3**(24) (2015), 1550020 (18 pages).
- [4] J. Cho, H. Kim and S. Kim, ‘Optimistic limits of Kashaev invariants and complex volumes of hyperbolic links’, *J. Knot Theory Ramifications* **10**(23) (2014), 1450049 (32 pages).
- [5] J. Cho and J. Murakami, ‘The complex volumes of twist knots via colored Jones polynomials’, *J. Knot Theory Ramifications* **11**(19) (2010), 1401–1421.
- [6] J. Cho and J. Murakami, ‘Optimistic limits of the colored Jones polynomials’, *J. Korean Math. Soc.* **3**(50) (2013), 641–693.
- [7] J. Cho and J. Murakami, Reidemeister transformations of the potential function and the solution. Preprint, 2015, [arXiv:1509.02378](https://arxiv.org/abs/1509.02378).
- [8] J. Cho, J. Murakami and Y. Yokota, ‘The complex volumes of twist knots’, *Proc. Amer. Math. Soc.* **10**(137) (2009), 3533–3541.
- [9] K. Hikami, ‘Generalized volume conjecture and the A -polynomials: the Neumann–Zagier potential function as a classical limit of the partition function’, *J. Geom. Phys.* **9**(57) (2007), 1895–1940.
- [10] K. Hikami and R. Inoue, ‘Braids, complex volume and cluster algebras’, *Algebr. Geom. Topol.* **4**(15) (2015), 2175–2194.
- [11] R. M. Kashaev, ‘The hyperbolic volume of knots from the quantum dilogarithm’, *Lett. Math. Phys.* **3**(39) (1997), 269–275.
- [12] F. Luo, S. Tillmann and T. Yang, ‘Thurston’s spinning construction and solutions to the hyperbolic gluing equations for closed hyperbolic 3-manifolds’, *Proc. Amer. Math. Soc.* **1**(141) (2013), 335–350.
- [13] C. T. McMullen, ‘The evolution of geometric structures on 3-manifolds’, *Bull. Amer. Math. Soc. (N.S.)* **2**(48) (2011), 259–274.
- [14] H. Murakami, ‘Optimistic calculations about the Witten–Reshetikhin–Turaev invariants of closed three-manifolds obtained from the figure-eight knot by integral Dehn surgeries’, *Sūrikaiseikikenkyūsho Kōkyūroku, Recent Progress Towards the Volume Conjecture*, Kyoto, 2000, 70–79 (in Japanese).
- [15] H. Murakami and J. Murakami, ‘The colored Jones polynomials and the simplicial volume of a knot’, *Acta Math.* **1**(186) (2001), 85–104.
- [16] H. Murakami, J. Murakami, M. Okamoto, T. Takata and Y. Yokota, ‘Kashaev’s conjecture and the Chern–Simons invariants of knots and links’, *Experiment. Math.* **3**(11) (2002), 427–435.
- [17] K. Ohnuki, ‘The colored Jones polynomials of 2-bridge link and hyperbolicity equations of its complements’, *J. Knot Theory Ramifications* **6**(14) (2005), 751–771.

- [18] H. Segerman and S. Tillmann, 'Pseudo-developing maps for ideal triangulations I: essential edges and generalised hyperbolic gluing equations', in: *Topology and Geometry in Dimension Three*, Contemporary Mathematics, 560 (American Mathematical Society, Providence, RI, 2011), 85–102.
- [19] Y. Yokota, 'On the complex volume of hyperbolic knots', *J. Knot Theory Ramifications* **7**(20) (2011), 955–976.
- [20] Y. Yokota, On the volume conjecture for hyperbolic knots. Preprint, 2000, [arXiv:0009165](https://arxiv.org/abs/0009165).
- [21] C. K. Zickert, 'The volume and Chern–Simons invariant of a representation', *Duke Math. J.* **3**(150) (2009), 489–532.

JINSEOK CHO, Pohang Mathematics Institute,
POSTECH, Gyungbuk 37673, Republic of Korea
e-mail: doi0425@gmail.com